Experimental assessment of an indirect method to measure the post-combustion flue gas flow rate in waste-to-energy plant based on multi-point measurements

Published Version:
Bellani, G., Lazzarini, L., Dal Pozzo, A., Moretti, S., Zattini, M., Cozzani, V., et al. (2023). Experimental assessment of an indirect method to measure the post-combustion flue gas flow rate in waste-to-energy plant based on multi-point measurements. WASTE MANAGEMENT, 157(2), 91-99 [10.1016/j.wasman.2022.12.004].

Availability:
This version is available at: https://hdl.handle.net/11585/912306 since: 2024-11-25

Published:
DOI: http://doi.org/10.1016/j.wasman.2022.12.004

Experimental assessment of an indirect method to measure the post-combustion flue gas flow rate in waste-to-energy plant based on multi-point measurements☆

Bellani G.[a,b], Lazzarini L.[a,b], Dal Pozzo A.[c], Moretti S.[e], Zattini M.[d], Cozzani V.[c], Talamelli A.[a,b]

[a] *Dipartimento di Ingegneria Industriale, Università di Bologna, Forlì, Italy*
[b] *Centro Interdipartimentale di Ricerca Industriale aerospaziale, Università di Bologna, Forlì, Italy*
[c] *Dipartimento di Ingegneria Civile, Chimica, Ambientale e dei Materiali, Università di Bologna, Bologna, Italy*
[d] *Essere S.p.A., Gruppo Ecoeridania, Forlì, Italy*
[e] *Arpae Emilia Romagna, Italy*

Abstract

In waste-to-energy plants, the determination of the flue gas flow rate in the post-combustion section is of the utmost importance, e.g., for the verification of the compliance to the minimum residence time requirements ($t_{res} > 2s$) or for the control of flue gas treatment reactant injection, but the harsh conditions (high temperature and content of pollutants) do not allow for a direct measurement. The present work reports an experimental assessment of an indirect approach to estimate the flue gas flow rate in the post-combustion section of a rotary kiln plant with reduced uncertainty. This method consists on the direct measurement of the flow rate at a "colder" section of the plant (the boiler outlet) combined to the simultaneous measurements of flue gas composition measurements upstream and downstream of the boiler. From these measurements it is then possible to determine the mass of false air and to retrieve the actual flue gas flow-rate in the post-combustion chamber. A massive experimental campaign has been conducted at a full-scale medical waste incinerator, in which flue gas flow rate was estimated at different waste loads and ambient conditions. The results show that

the percentage of false air can be significant and simply neglecting it can lead to substantial under-performance of the plant. Issues related to the practical implementation of the methods are illustrated in detail and the possibility to extend the methodology towards an online determination of post-combustion flue gas flow rate is discussed.

Keywords

Waste combustion, Fluid dynamics, residence time, Experimental campaign, PCDD

1. Introduction

Increasing restrictions on emissions and more ambitious targets on energy recovery are driving waste-to-energy (WtE) plants towards higher levels of process optimization (De Greef et al. 2013); (Eboh et al. 2019,Liu et al. 2020). To this purpose, modern facilities typically collect hundreds of process data via a wide array of sensors and measuring devices (Birgen et al. 2021). The diffusion of data mining approaches has significantly improved the capability to harness this wealth of information to improve the control of process operation (Bacci di Capaci et al. 2022, Dal Pozzo et al. 2021, Magnanelli et al. 2020).

In this framework, a quantity of great interest is the flue-gas flow-rate (FGFR) generated by waste combustion in the chamber of a grate furnace or in the post-combustion chamber of a rotary kiln. The latter is of special interest because of the restrictive norms that regulate the residence time of the flue-gas. In terms of process control, having an accurate direct or indirect online measurement of the FGFR may significantly improve the control of the feed-rate of reactants injected directly in the combustion chamber for flue gas cleaning, e.g. the furnace injection of dolomitic sorbents (Biganzoli et al. 2015, Dal Pozzo et al. 2020). With respect to the compliance to environmental regulations, in Europe a minimum residence time of 2 s at 850°C is required for flue gas resulting from waste incineration (Directive 2010/75/EU), to ensure the full thermal destruction of organo-halogenated compounds either released by the waste or formed in low-temperature spots during combustion (Chen et al. 2015; Caneghem et al. 2014). Clearly enough, in order to monitor the compliance with this requirement, FGFR needs to be evaluated.

Measurement of WtE FGFR is mandatory at the stack of the plant, but this value might significantly differ from the FGFR generated in the combustion chamber as a consequence of air infiltration in the boiler and in the flue gas cleaning line (Dzurňák et al. 2020). Further uncertainties may derive from the variation in the water vapour concentration in flue gas, depending on the use of wet techniques for flue-gas treatment (Dal Pozzo et al. 2018, Poggio & Grieco 2010). One possible approach is to simply disregard this contamination and make a conservative estimation of the residence time based on stack data. However, if the extent of false air is significant, this assumption can be overly conservative and it can lead to a sub-optimal management of the plant and/or, ultimately to tensions between the plant operator, the regulator and the public opinion.

Unfortunately, a direct measurement of flowrate at the exit of combustion chamber is generally not possible, as the standardized method based on a grid of point velocity measurements made with Pitot tubes (EN 16911/13 2013) is unfeasible due to the extremely high temperatures and harsh conditions of this section of the plant (Klopfenstein Jr 1998). Even the aforementioned Directive 2010/75/EU, while stating that the residence time requires appropriate verification, does not provide indication on how such determination should be performed (Stålnacke et al. 2008).

In industrial practice, monitoring of residence time relies upon semi-empirical algorithms implemented in the Distributed Control System (DCS) that derive local variables from measurements obtained downstream in the flue-gas cleaning line (Costa et al.

2012). For example, Eicher 2000 proposed a procedure to estimate gas-phase residence time in the combustion chamber based only on the combustion chamber temperature and stack-gas data. However, such algorithms are not standardized (Viganò & Magli 2017) and, in order to give reliable estimates, they require calibration data obtained by ad-hoc full-scale test runs on the operating plant.

The aim of the present study is to assess a methodology to determine the FGFR of the post-combustion chamber of a rotary kiln hazardous waste incinerator through a massive experimental campaign on a full-scale medical-waste plant. The data collected in this campaign allows us to quantify the amount of false-air infiltration and its relevance for the overall estimation of flue-gas flow rates of the plant. The proposed method is based on the measurements of the main volumetric composition of the gas (*i.e.* mainly CO_2, O_2 and H_2O) and on the gas velocity downstream of the post-combustion chamber, at the exit of the boiler section, where the gas temperature allows direct velocity measurements. The concentration data are then elaborated to derive the flow-rate corrections from mass balance of the main volumetric components of the gas. In this paper we discuss the theoretical framework of the method, the methodology for its practical implementation and the data from the validation campaign in a full-scale medical-waste plant operating at load and ambient conditions covering the entire operative range. In light of these results, we discuss the potential application of this method to online FGFR estimation based on the available plant data.

2. Material and methods

2.1. Reference case

The case-study presented here is the experimental validation of an indirect method to determine the mass flow rate of the flue gas in the post-combustion chamber of an hazardous waste incinerator with rotary kiln. Figure 1a shows the typical configuration of the combustion and heat recovery section of this type of WtE plant.

As shown in the figure, the post-combustion chamber is positioned immediately after the kiln. The flue gas leaving the post-combustion chamber (section 1 in Figure 1a) enters the steam generator (heat-recovery section of the plant). Here, the gas temperature typically decreases from $1000^\circ C$ to about $200 - 250^\circ C$. Downstream of the steam generator (section 2 in Figure 1a), the cold gas flows freely in a regular duct before entering the next flue gas treatment sections. If the circuit were perfectly sealed, flue gas flow rate and residence time in the post-combustion chamber could be directly estimated via mass flow measurements in section 2. However, due to constructions constraints, infiltration of ambient air typically occurs in the steam generator, therefore mass-flow measurements in section 2 are biased and typically lead to a substantial overestimation of the mass-flow in the post-combustion chamber.

Here we introduce a correction method based on the mass balance evaluated thanks to the simultaneous measurements of gas volume-fractions at the upstream and downstream end of the steam generator, as well as the experimental procedure to experimentally evaluate this correction.

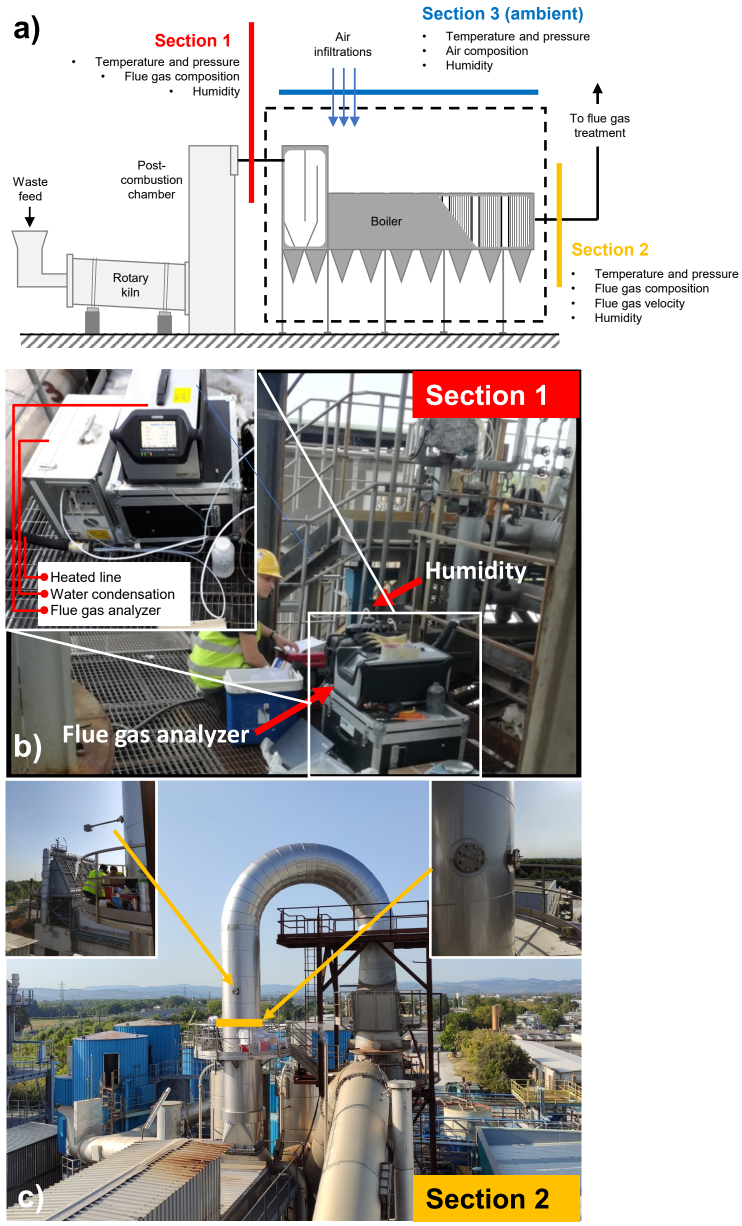

Figure 1: (a) Schematic the incinerator layout: waste enters on the bottom left inside the rotary kiln, at the top of the post-combustion chamber temperatures of the flue gas reach up to $1000^{\circ}\,C$; measurement section 2 is placed after the steam generator and the upward 90° corner, here flue gas temperature decreases approximately to $200-250^{\circ}\,C$; Section 3 indicates ambient condition as close as possible to the post-combustion chamber.(b) Instrumentation placed in section 1. In the inset it can be seen the gas analyzer used to monitor flue gas concentration and the humidity sensor (c) location of the control point and of the measurement grid in section 2 is highlighted by the yellow arrows; red arrows indicates the flue gas direction.

2.2. Methodology

The method is based on the following procedure: a) evaluation of the gas flow rate in the "cold" section (section 2 in Figure 1a); b) measurement of the composition of the flue gas in section 1 and section 2, measurement of the ambient condition in section 3; c) solution of the mass balance in the boiler based on the measurements of gas composition and quantification of the correction term for the indirect estimate of the gas flow rate in the "hot" section (section 1 in Figure 1a). More specifically, once obtained volumetric flow rate in section 2, the mass-balance based on the volumetric concentration measurements in sections 1 (post-combustion), 2 (cold section) and 3 (ambient) can be written as:

$$\dot{m}_1 = \dot{m}_2 - \dot{m}_3, \tag{1}$$

which is convenient to express in terms of volumetric flow-rate and density:

$$\rho_1 \dot{Q}_1 = \rho_2 \dot{Q}_2 - \rho_3 \dot{Q}_3. \tag{2}$$

Writing the balance separately for the components O_2 and CO_2 in the dry flue gas the following system is obtained:

$$\begin{cases} \dot{Q}_{1d} \left[\frac{p_1}{RT_1}(M_{O_2}\varphi_{1,O_2})\right] = \dot{Q}_{2d} \left[\frac{p_2}{RT_2}(M_{O_2}\varphi_{2,O_2})\right] \\ \qquad\qquad\qquad\qquad - \dot{Q}_{3d} \left[\frac{p_3}{RT_3}(M_{O_2}\varphi_{3,O_2})\right] \\ \dot{Q}_{1d} \left[\frac{p_1}{RT_1}(M_{CO_2}\varphi_{1,CO_2})\right] = \dot{Q}_{2d} \left[\frac{p_2}{RT_2}(M_{CO_2}\varphi_{2,CO_2})\right] \\ \qquad\qquad\qquad\qquad - \dot{Q}_{3d} \left[\frac{p_3}{RT_3}(M_{CO_2}\varphi_{3,CO_2})\right] \end{cases}$$

Solving now the system for $\dot{Q}_{1d}$ it is possible to obtain the dry volumetric flow rate of the flue gases in section 1:

$$\dot{Q}_{1d} = \dot{Q}_{2d} \left[\frac{\frac{p_2}{T_2}(\varphi_{2,O_2}\varphi_{3,CO_2} - \varphi_{3,O_2}\varphi_{2,CO_2})}{\frac{p_1}{T_1}(\varphi_{1,O_2}\varphi_{3,CO_2} - \varphi_{3,O_2}\varphi_{1,CO_2})} \right], \tag{3}$$

where the term in square brackets represents the correction term due to ambient air infiltration as determined by the differences in volume concentrations and thermodynamic variables (namely pressure and temperature). In order to obtain the wet volumetric flow rate, the vapour fraction φ_{1,H_2O} in the duct must also be taken into account. Thus the expression for the wet volumetric flow rate can be computed as:

$$\dot{Q}_{1,w} = \dot{Q}_{1,d} \frac{100}{100 - \varphi_{H_2O,1}}; \tag{4}$$

Once the wet volumetric flow-rate has been computed, the mean residence time of the flue gases in the post-combustion chamber (t_{res}) can be expressed as:

$$t_{res} = \frac{V_{PC}}{\dot{Q}_{1,w}}, \tag{5}$$

where V_{PC} is the effective volume of the post-combustion chamber.

2.3. Experimental setup and procedure

The methodology outlined in section 2.2, derived from fundamental conservation laws, requires the experimental evaluation of the flue gas flow rate in section 2 ($\dot{Q}_{2d}$) and of temperature, pressure, and concentration of O_2, CO_2, H_2O in sections 1, 2 and 3 (ambient conditions). The determination of these quantities in the operating conditions of a WtE plant poses specific challenges.

In particular, the first challenge concerns the evaluation of $\dot{Q}_{2d}$. Assuming a circular duct, gas flow rate in section 2 is defined from the following double integral:

$$\dot{Q}_{2d} = \int_0^{2\pi} \int_0^r v_c(r, \Theta) dr \cdot r d\Theta \cdot (1 - \varphi_{2,H_2O}) \tag{6}$$

where $\dot{Q}_{2d}$ is the gas flow rate in section 2, dry; r is the radius of the pipe line; $d\Theta$ represent the chosen polar coordinate and v_c is the measured velocity of the flue gases. The coefficient $(1 - \varphi_{H_2O,2})$ accounts for the wet volume fraction $(\varphi_{H_2O,2})$ in section 2.

The directive UNI EN 16911/13 (EN 16911/13 2013) requires that flow-rate measurements must be performed at a straight circular duct sufficiently long (at least 7 diameters: minimum 5 upstream and 2 downstream of the measurement section) to guarantee nearly uniform and symmetric velocity profiles at measurement location. In this condition, the directive requires to measure the velocity at 7 measurement points along 2 diameters.

However, this is not always available in operating plants. This means that velocity profiles may present substantial asymmetries (Kalpakli et al. 2013) and evaluating $\dot{Q}_{2d}$ on a standard course grid may be a significant source of inaccuracies. Therefore, a correct evaluation of $\dot{Q}_{2d}$ requires the acquisition of the flue gas velocity in multiple points, an operation that requires a significant amount of time. For the time needed to measure the velocity in each point of the grid, the plant needs to be operated at a constant feed rate of waste, in order to maintain a relatively constant flow rate of the flue gas.

On the other hand, the other variables required by the methodology (temperature, pressure and concentrations in eq.(3)) need to be evaluated at higher rates for statistical reasons (see section 2.4). In general, their measurements might not be synchronized with the velocity measurements, thus a well-defined interpolation and averaging procedure needs to be defined. In this work, a dedicated experimental campaign at a full-scale plant was carried out to test specific solutions to the aforementioned technical challenges and to validate the proposed methodology.

The experimental campaign was conducted at the medical waste incinerator "Essere S.p.A," in Forlì (Italy). The plant has the layout in Figure 1a. The rotary kiln for waste combustion is followed by a $125\,m^3$ cylindrical adiabatic post-combustion chamber. The flue gas that leaves the chamber at temperatures of about $1000\,°C$ (first measurement section, S1, on top of the chamber) enters a $11.18MW$ steam generator. The steam generator is 25 m long and kept at lower than atmospheric pressure to avoid flue gas leakage. As a consequence, as discussed before, ambient air can penetrate from the exterior and mix with the flue gas, increasing its O_2 concentration and decreasing its CO_2 concentration. At the boiler exit the flue gas has cooled to approximately $250\,°C$ and enters a vertical circular duct through an upward 90-degrees corner. The second measurement section (S2) is placed 2.7 diameters downstream this corner and ≈ 2.5 diameters upstream of the 180-degree corner (see figure 1). This section is the closest zone to the post-combustion chamber which presents flow condition that allows direct measurements of differential pressure through a standard Pitot-s probe. In principle, the method of flue gas flowrate estimate based on the mass balance introduced in section 2.2 can be applied using any downstream section of the flue gas line as section S2. The choice to remain closest to the post-combustion chamber was made to avoid other interferences on flue gas composition, other than air infiltrations, that take place downstream in the flue gas cleaning line and can add uncertainty to the estimate of the correction term in eq.(3). For the reference plant, such interferences included changes in water vapour content due to wet scrubbing for HCl/SOx removal and, to a lesser extent, changes in CO2 concentration due to uptake by hydrated lime injected for HCl removal Dal Pozzo et al. 2018.

Although the conditions in S2 are closest to the one imposed by the standard UNI-

EN 16911/13 2013, it is well known that a 90-degree corner produces strong asymmetry in the flow (Kalpakli et al. 2013). To account for this, an higher resolution for the acquisition of velocity data was pursued and a refined measurement grid of 44 logarithmically-spaced points on 4 evenly spaced diameters was adopted (see Fig.2a). For each grid point, the flue gas velocity measured with a Pitot-S was sampled for 15 s. This time was chosen to minimize statistical uncertainty while keeping the total measurement time below 60 min, a duration in which it was possible to operate the plant at a reasonably constant flue gas flow rate. To monitor the stability of the flue gas flow rate during the measurement, a second Pitot-S probe was positioned at the center of the duct, 1 m downstream of S2 (control point). The position of the probes are manually controlled through specifically designed flanges.

At sections S1 and S2, as well as in ambient air outside the steam generator (S3), pressure, temperature, O_2 and CO_2 concentrations were monitored at a rate of one sample per minute for the entire duration of the experiments. Pressure was measured with a differential pressure transducer (2.5 kPa range, 1% full-scale accuracy). The temperature sensor is a k-type thermocouple of 0-1200 °C range for section 1, whereas j-type thermocouple for sections 2 and 3. The concentrations of CO_2 and O_2 in the dry gas were measured by non-dispersive infrared absorption and paramagnetic method, respectively. Finally, the average volumetric concentration of water vapor in the gas was measured in all sections for each experiment by the standard condensation/absorption technique (EN 14790/17 2017). The sampling time of each instrument was set to be larger than their respective time-response. Data-rates, instrument types and relative accuracy are summarized in table 1.

Parameter	Frequency [Samples/min]	Instrument	Accuracy	Time response
S1				
$\varphi_{1,0_2}$	1	Gas analyzer PG-300 Horiba	±1%	45 s
$\varphi_{1,C0_2}$	1			
φ_{1,H_2O}	single sampe	Gravimetric test	±3%	1 hr
$T1$	1	type k thermocouple	±1%	NA
$p1$	1	Digital stack gas velocity		
S2				
$\varphi_{2,0_2}$	1	Gas analyzer PG-300 Horiba	±1%	45 s
$\varphi_{2,C0_2}$	1			
φ_{2,H_2O}	single sampe	Gravimetric test	±3%	1 hr
$T2$	1	type j thermocouple	±1%	NA
$p2$	1	Digital stack gas velocity		
v_k	manual sampling	Pitot - S	±1%	
v_{fC}	1			
S3				
$\varphi_{3,0_2}$	1	Gas analyzer PG-300 Horiba	±1%	45 s
$\varphi_{3,C0_2}$	1			
φ_{3,H_2O}	single sampe	Gravimetric test	±3%	1 hr
$T3$	1	type j thermocouple	±1%	NA
$p3$	1	Digital stack gas velocity		

Table 1: Summary of the instrumentation used to measure the relevant parameters with the corresponding sampling frequency, accuracy and time response. The accuracy is the one specified by the instrument manufacturer.

2.4. Data processing and averaging

As discussed in section 2.3, to determine the volumetric flow rate in section 2 we must evaluate the integral as defined by eq. (6). We define the index $k = 1 : 44$ corresponding to the $k-th$ Pitot-S measurement. At each k is associated the corresponding measurement point on the grid and time-interval in which the data is taken.

The velocity of the flue gas v_k is computed as follows:

$$v_k = \sqrt{\frac{2\Delta p_k}{\rho_{2,k}}}, \tag{7}$$

where Δp_k is the k_{th} 15s-average differential pressure measured by the Pitot-S. The variable $\rho_{2,k}$ is the density of the flue gas determined according to the following expression:

$$\rho_{2,k} = \frac{p_k}{RT_k}[M_{O_2}\varphi_{2,k,O_2}+M_{CO_2}\varphi_{2,k,CO_2}+M_{H_2O}\varphi_{2,k,H_2O}+M_{N_2}(1-\varphi_{2,k,O_2}-\varphi_{2,k,CO_2}-\varphi_{2,k,H_2O})], \tag{8}$$

where M_x is the molar mass of the element x, $\varphi_{2,k,x}$ is the volume concentration of the element x measured in S2 at time interval k, p_k and T_k are the local pressure and temperature at time-interval k and R is the molar gas constant equal to 8.31446 expressed in $[J/Kmol]$. The average volume flow rate $\dot{Q}_{S_2}$ is computed by numerically solving the integral of eq. (6) according to the trapezoid rule. Since $\dot{Q}_{2,d}$ represents a single average value of the volume flow-rate over the time interval needed to span the entire grid, the correction term expressed in eq. (3) must be averaged as well. Since the volumetric concentrations are not independent variables, the correction term cannot be computed after averaging the individual terms (Bendat & Piersol 2000) but as global average of the instantaneous combination of each variable, according to the following expression:

$$\dot{Q}_{1d} = \dot{Q}_{2d} \cdot \sqrt{\left[\frac{\frac{p_2}{T_2}(\varphi_{2,O_2}\varphi_{3,CO_2} - \varphi_{3,O_2}\varphi_{2,CO_2})}{\frac{p_1}{T_1}(\varphi_{1,O_2}\varphi_{3,CO_2} - \varphi_{3,O_2}\varphi_{1,CO_2})}\right]}. \quad (9)$$

It must be pointed out that a potential source of uncertainty is given by the time delay between the measurements in S1 and S2. The effect of the time delay is to reduce the correlation coefficient between the quantities measured in S1 and S2, thus altering the balance expressed in eq.(9). However, in the present configuration, the estimated time-delay is between 1-3 s for all cases, which is much smaller than both the sampling interval and the characteristic time-scales of the flow. Therefore, it can be considered negligible. This is also confirmed by the fact that the correlation coefficient of the corresponding signals is found to be between 0.6 and 0.9 in all cases. More details on the choices of sampling parameters, measurement grids and associated experimental uncertainties are given in the supplementary material.

2.5. Experimental campaign

In order to test the methodology over a wide range of operating conditions of the plant and extract relevant trends, experiments were performed at three different levels of waste loading, corresponding to the lowest (Low: ≈ 2700 kg/h), intermediate (Medium: ≈ 3800 kg/h) and nearly maximum loading (High: ≈ 4800 kg/h) capability of the plant. Each test was at least 1-h long and, in addition to a controlled waste feed rate, also the air feed rate to the kiln was maintained as constant as possible during the tests to reduce its influence in the estimate of the FGFR. To test the robustness of the results in different ambient conditions, the same three cases were repeated at 6 months interval from each other (in summer and winter). Therefore, we have divided the results in 6 test cases, namely: SL, SM, SH and WH, WM, WL; where L, M and H stands for low, medium and high loading conditions, respectively, while S and W indicate summer and winter sessions, as shown in table 2.

3. Results and discussion

Case	Load $[kg/h]$	$Q_{2,d}$ $[m^3/s]$	$Q_{2,w}$ $[m^3/s]$	Q_2 $[Nm^3/h]$	φ_{2,H_2O} [%]	$Q_{1,d}$ $[m^3/s]$	$Q_{1,w}$ $[m^3/s]$	Q_1 $[Nm^3/h]$	φ_{1,H_2O} [%]	t_{res} $[s]$
SL	2700	14.20	17.30	34512	17.88	27.61	34.54	26759	20.05	$3.62 \pm 2.74\%$
WL	2868	13.10	15.23	30742	13.97	26.85	31.99	23723	16.08	$4.06 \pm 2.72\%$
WM	3770	15.62	19.30	38081	19.06	26.51	33.72	25821	21.36	$3.71 \pm 2.66\%$
SM	3910	17.03	18.87	36420	NA	*29.87	*36.40	NA	NA	$*3.14 \pm 2.70\%$
SH1	4684	20.15	23.31	43705	NA	*33.20	*40	NA	NA	$*2.70 \pm 2.63\%$
SH2	4700	19.49	23.51	44310	17.08	36.12	44.93	34374	19.61	$2.78 \pm 2.59\%$
WH	4770	19.15	22.67	42930	15.53	34.69	42.90	30412	19.12	$2.91 \pm 2.74\%$

Table 2: Loading conditions and estimated flow rates for each of the six different tested conditions; $\dot{Q}_{2,d}$ and $\dot{Q}_{2,w}$ shows respectively the dry and wet gas flow rate measured in section 2, $\dot{Q}_2$ represent the FGFR in standardized condition; $\dot{Q}_{1,d}$ and $\dot{Q}_{1,w}$ represents respectively the dry and wet gas flow rate evaluated in post combustion chamber; $\dot{Q}_1$ shows the FGFR in standardized condition; φ_{i,H_2O} show the humidity for sections 2 and 1 respectively; t_{res} shows the residence time of the flue gas in post-combustion chamber. The cases SM and $SH1$ have been discarded because of incoherent data. The case SH has been repeated in order to obtain valid data at the highest loading condition. The sub-indexes $SH1$ and $SH2$ have been introduced to identify the discarded and the valid test, respectively; *, NA:data acquired during tests SM and SH1 were recovered using the mean infiltration coefficient and the mean humidity values measured in the remaining experimental campaigns.

3.1. Data assessment and validation

Given the challenging conditions in which the experiments are performed (*i.e.* extreme temperature, corrosive gas, dust particles, unknown fuel composition, etc) a careful preliminary assessment of the consistency of the data is needed. The first assessment concerns the hypothesis of statistical stationariety of the plant conditions. This is done by analyzing the timeseries of the velocity measured at the control point, looking for possible trends or anomalous fluctuations indicating for non-stationariety of the plant operating conditions.

Figure 2(c) shows a time trace of the control point for one of the cases. Analysis of the time-series for all cases show that despite the variability of the fuel composition during each test, the plant operates at reasonably constant conditions since no significant trends or bursts are observed. Furthermore, the standard deviation of the velocity fluctuations normalized by the value of the local mean are within 5%, a value that is comparable with the expected level of turbulent fluctuations in the centre of a circular duct (Fiorini et al. 2017; Willert et al. 2017). Given the stationary conditions of the plant, the next step of the procedure is the calculation of the gas flow rate in section 2 by integration of the velocity profiles along the diameters shown in figure 2a.

Considering that the measurement section is located downstream of a 90° bend, the flow is not expected to be canonical (*i.e.* fully-developed pipe flow), therefore, there are no analytical or empirical formulas to describe the expected velocity profiles. However, it is well known that in a corner the radial pressure gradient produces strongly asymmetric profiles except in the direction parallel to the rotation axis (D1 in the present case)(Kalpakli et al. 2013). Figure 2c shows that the measured profiles are consistent with the expected behaviour.

Furthermore, velocity profiles scaled by the centerline velocity or by the average velocity are expected to have a substantially self-similar shape (i.e. independent of

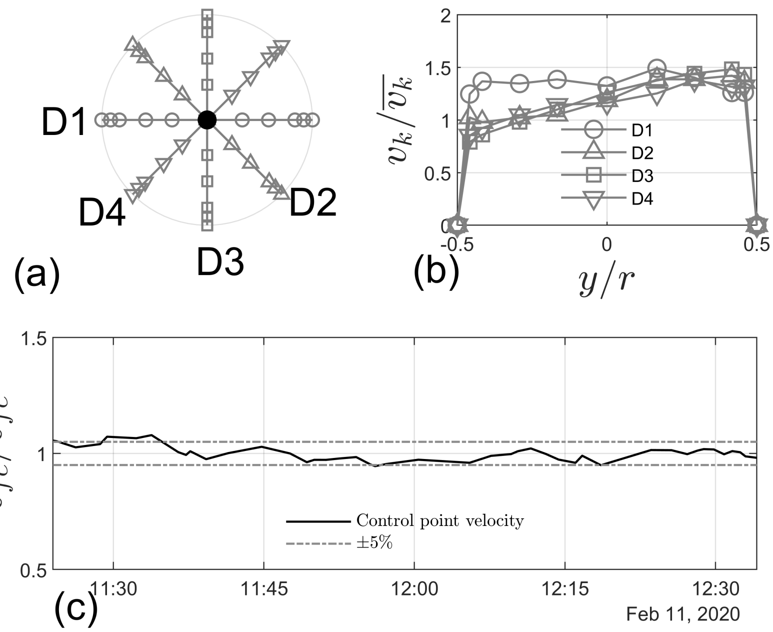

Figure 2: (a) represents the measurement grid used in S2, each diameter has 9 measurement points spaced logarithmically from the wall to the center line. The physical coordinates of the measurement points expressed as a fraction of the duct radius are: -0.4583, -0.4167, -0.2917, -0.1667, 0, 0.1667, 0.2917, 0.4167, 0.4583. the central black dot shows the position of the control point placed 1 meter downstream with respect to the measurements grid; (b) depict the shape of the velocity profiles measured starting from D1 to D4 and normalized with the mean velocity of the entire test, the dimension of each symbols reflects the actual standard deviation associated to the correspondent measurement point; the mean value of the standard deviation is of the order of 6-7% (c) shows the behaviour of the control point velocity during a winter test normalized with the mean velocity of the entire test.

the average speed itself). This normalization allows us to compare profiles related to different flow conditions and to compute mean scaled velocity profiles for the winter and summer sessions averaging the corresponding profiles for the three cases of each season. These averaged velocity profiles are shown and compared in figure 3. The substantial agreement between the two sessions is an indication of the consistency of the experimental procedure.

The final assessment is done on the gas volumetric composition data. These measurements are especially challenging in section S1 due to the highly aggressive environment. In these section, partial probe occlusions (e.g., by deposition and melting of

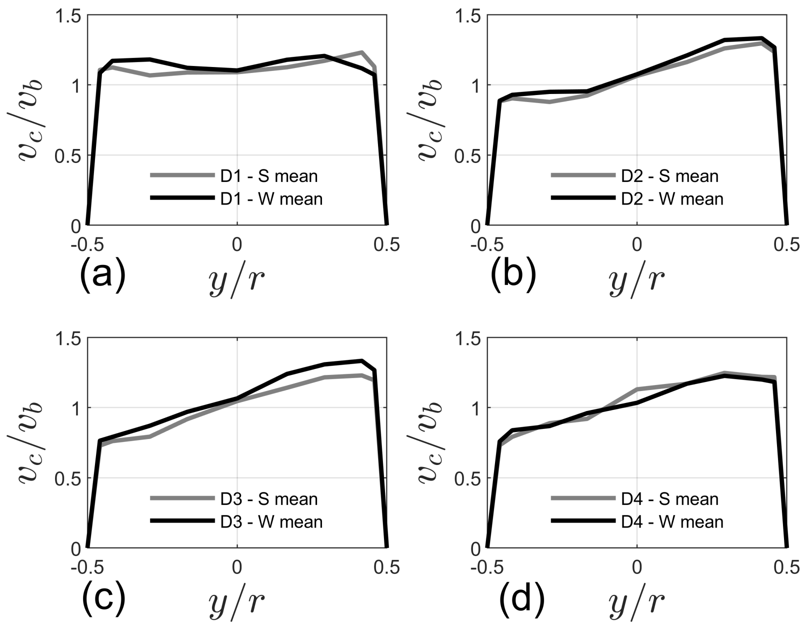

Figure 3: Normalized (with bulk velocity and pipe radius) mean velocity profile divided in diameters; D1 in figure (a), D2 in figure (b), D3 in figure (c) and D4 in figure (d), in grey the summer experiments whereas in black the winter experiments.

combustion fly ash) can cause significant biases in the measurements, therefore a check of the consistency of these measurements is essential. To this purpose, we impose a constraint based on a mass balance between CO_2 and O_2. The concentration of these two species in the flue gas from combustion processes is anti correlated, as combustion consumes O_2 and produces CO_2 according to an exchange ratio or oxidative ratio (defined as $-\Delta O_2\ /\Delta CO_2$) that depends on the elemental composition of the fuel (Seibt et al. 2004). Such ratio lies in the range $1.1 - 1.3$ for solid fuels of diverse nature (Keeling & Manning 2014; Lueker et al. 2001). Therefore, even if the waste composition fed to the incinerator is relatively heterogeneous, it was found that for most of the data collected during the experimental campaign the volumetric concentration of CO_2 plotted against that of O_2 returned a linear correlation (see Figure 4), corresponding to an average oxidative ratio of 1.25. Notably, the data from two tests (SM and SH1), indicated by the gray triangles deviated significantly from the trend, pinpointing a possible instrumental error. Given that a reliable determination of the volumetric concentrations is key for the entire procedure, these cases were marked as “discarded” cases. The SH case was repeated after the probe had been cleaned from occlusions and the following measurements show good agreement with the expected trend (see diamonds in the figure).

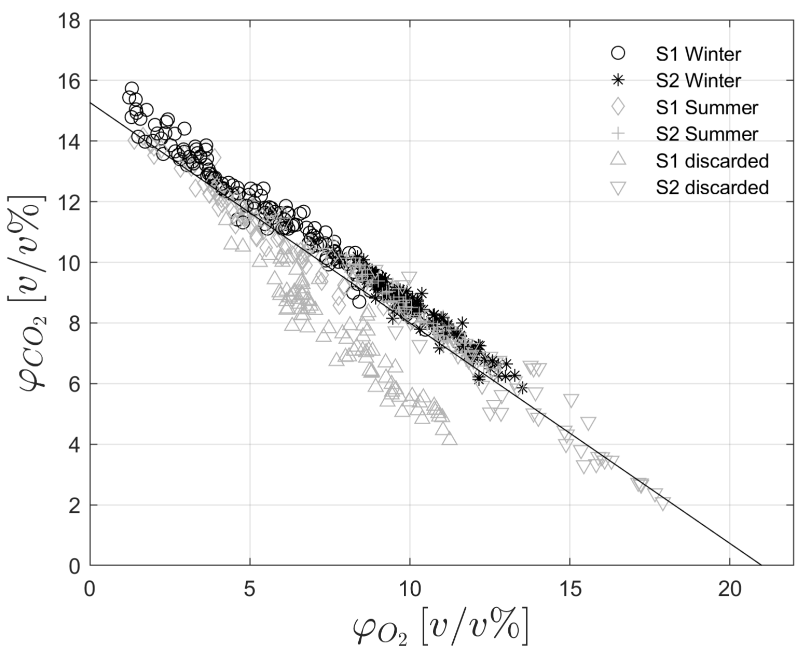

Figure 4: Volumetric gas composition, CO_2 Vs. O_2. Each point represents a measurement conducted during the tests (time resolution 60 s) The black circles represent the winter data in S1, the grey diamonds represent the summer data in S1, the black asterisks represent the winter data in S2, the grey cross represents the summer data S2, the gray triangles represent discarded data due to instrumentation fault in S1.

3.2. Flow-rate measurements

Once the data have been validated, it is possible to proceed with the numerical integration of the velocity profiles measured in S2 in order to determine the dry volumetric flow rate of the flue gases, as defined in equation 6. Figure 5 (a) shows the measured dry flow rate values in S2 plotted against the waste feed-rate. The figure shows a nearly-linear increasing trend as the waste feed-rate increases. For the purpose of estimating the repeatability of the measurements, also the cases who did not pass the validation of the volumetric concentration measurements were included, since these did not affect the measurement of $Q_{2,d}$. It can be noticed a substantial agreement between summer and

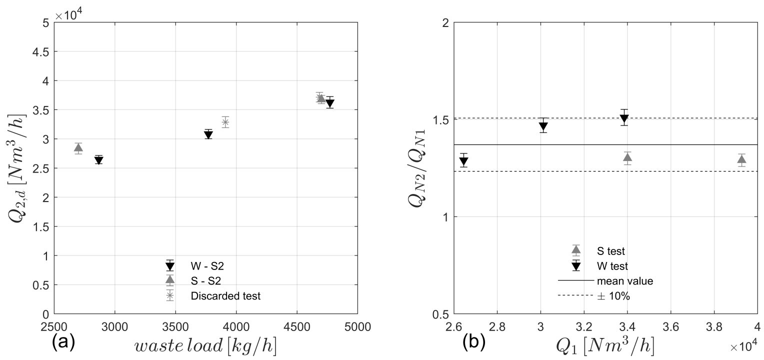

Figure 5: (a) Dry gas flow rate in section 2. Summer and winter tests are shown by black and grey symbols, respectively. The grey asterisk symbols are the discarded cases (SM1 and SH1). Error bars is the estimated measurements uncertainty. (b) Infiltration coefficient expressed using mass flow rate in S1 and S2. black downward triangles represents the winter experiments, grey upward triangles represents the summer experiments, black line highlight the mean value of the coefficient while dashed black lines shows a $\pm 10\%$ with respect to the mean value.

winter measurements, especially at medium and high waste load, while a slightly larger scatter is present at low load. Considering that waste is a highly heterogeneous fuel, it can be expected that at low waste feed rates the statistical variability in combustion behaviour given by different waste fractions is magnified.

In order to evaluate flow rate in S1 the infiltration through the steam generator needs to be quantified according to equation 9. Figure 5 (b) shows the infiltration coefficient expressed as the ratio between Q_{2N}/Q_{1N} where Q_{2N} and Q_{1N} represent the volume flow rates in S2 and S1, respectively, with density at standard air conditions.

The mean value of the infiltration coefficient is of 1.38 $\pm 10\%$. This value shows that the amount of false air entrained in the boiler section only is hardly negligible being nearly 40% of the total mass flow rate. This percentage increases even more if the volume-flow rate (to which the residence times are proportional) is considered, given the density ratio between the cold section and the post-combustion chamber.

The higher extent of variation of the infiltration coefficient observed in winter can be explained by the fact that the scheduled annual maintenance of the steam generator was carried out just before the summer tests. Therefore, the winter tests were done in presence of an higher degree of fouling and occlusions in the boiler, which is compatible with a higher duty for the induced-draft fan and thus to a higher differential pressure. This condition is therefore compatible with the higher value of dilution observed.

3.3. Residence time

Figure 6a shows that the trend observed for Q_{S2} is confirmed also by the wet volumetric flow rate, computed according to equations (3) and (4). The asterisks in the figures are the cases originally discarded because of unreliable flue gas composition measurements and humidity measurements. For these cases, it was not possible to directly compute the infiltration coefficient, therefore, instead of the direct measurement, the mean value of the measured coefficients (*e.g.* 1.38) has been taken. The same approach was followed for the humidity, as the mean value of the humidity measured in all cases in S2 and S1 respectively, was used. The resulting flow-rates follow remarkably well the trend of the measured values.

In order to check if the measured values are consistent with the plant design, it is interesting to convert $Q_{1,w}$ into residence times according to eq. (5). The reference volume used for this calculation is of $125.1\,m^3$. Based on this expression, the evolution of residence time as a function of the plant waste-loading is shown in figure 6 (b); The

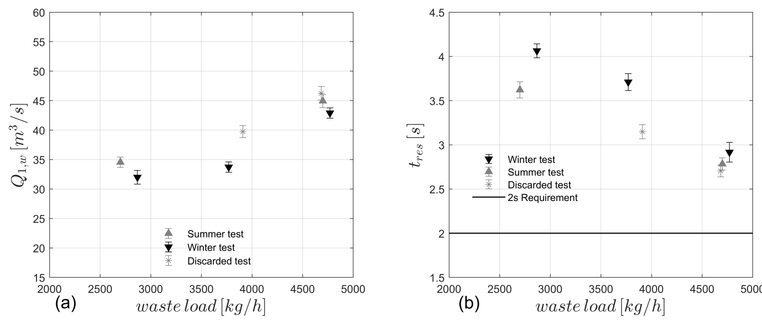

Figure 6: (a) wet gas flow rate calculated for S1, (b) t_{res} of the flue gas in post-combustion chamber. grey error-bar represents summer experiments, black error-bar represents winter experiments, asterisks represents the discarded experiments. These cases have been recovered using the average infiltration coefficient and the average humidity measured in all cases. Black line represents the 2 seconds requirement.

figure shows that as the waste feed rate approaches its design limit (5000 kg/h), the residence time gets close to the two-seconds limit with a margin of about 40% against an estimated uncertainty on the single measure of the order of 2.5% (see supplementary material). Assuming that the plant is designed to respect the norm, the fact that the estimated residence times are close but higher than the prescribed value of 2s at nearly the maximum operative range of the plant can be considered an indirect assessment of consistency of the results obtained in the entire campaign. Furthermore, it is interesting to notice that without the corrections for false air entrainment, given its extent, it may appear that the plant is violating the norm of the 2s residence times, thus a reduced operational range should be imposed.

3.4. Discussion

Despite the simplicity of the theoretical procedure devised to estimate the FGFR in the post-combustion chamber, its experimental implementation implied numerous issues that needed to be addressed with a massive experimental campaign. The main issues were: stability of plant operation during the tests, consistency of the velocity profiles, and reliability of the volumetric concentration measurements in all operating conditions.

Regarding the possibility to operate the plant in stable conditions, the data collected in the control point showed that no significant trends or anomalous bursts were observed. This confirms the main assumption that the flow-rate is statistically stationary during each measured case (as already observed in the preliminary tests, see supplementary material). The stability of the flow conditions is also confirmed by the substantial repeatability of the results over independent measurement sets collected in different period of the year with possible influences of fuel seasonal variability and different ambient conditions (*i.e.* winter and summer season, see fig. (3)).

Another important finding is that the velocity profiles are self-similar when scaled by the radius and the centerline velocity. This finding has two relevant implications: on one hand this can be used to evaluate the accuracy of the individual velocity measurements by looking at the deviation from the overall mean. This was found to be below 10% for all cases, and it reduced to 5% for the cases with an improved control of the S-probe position; Most importantly, self-similarity of the velocity profiles in $S2$ section point at the possibility of estimating the flow-rate from a single-point measurement.

A crucial part of the procedure is the volumetric concentration measurements. A small bias in this measurements can lead to significant errors in the estimation of the FGFR. The diagnostic plot shown in figure 4 has proven to be a robust tool to validate these measurements and produce a consistent estimation of the infiltration of fresh air through the steam-generator. Further work should be done in order to explore the influence of non-ideal burning conditions on the diagnostic plot, and additional checks, such as the correlation coefficients between the four signals could be introduced.

However, the consistency of the present results in terms of infiltration coefficient (see figure 5(b)) and the estimated residence time near to the 2 s limits at the design point of the plant (see figure 6 (b)), obtained in a variety of operating conditions, are encouraging.

The obvious limit of the methodology presented here is that it does not allow obtaining instantaneous FGFR estimates. However, the experimental data presented here provide a solid ground to prospect an extension of the present methodology towards real-time estimation method. In particular, based on the results we can outline the following revised procedure that would require minimal plant modification: a) Exploit self-similarity of velocity profiles to obtain the volumetric flow rate of the cold section with velocity measurements in a single point. b) Estimate an instantaneous or average infiltration coefficient from CO_2 and O_2 online measurements; c) Compute dry volumetric flow rate in the hot section based on the infiltration coefficient; d) Estimate the wet flow rate based on the typical mean value of the water vapour concentration in the flue gas.

Alternatively, a plant operator might consider setting up a different algorithm for real-time FGFR estimate in the post-combustion chamber exclusively based on existing process instrumentation (e.g., estimate from online flue gas composition measurements at stack or from energy balance in the heat recovery section of the plant). Any algorithm for FGFR estimate based on indirect measurements of other variables through existing process instrumentation or ad-hoc sensors would require a training and validation campaign. The present methodology offers the possibility to obtain average estimates of FGFR in the post-combustion chamber under different operating conditions that can be used as the necessary dataset for the training and validation of such algorithms.

Lastly, it is worth recalling that this paper demonstrated the methodology in application to a specific, albeit relevant, case of WtE plant: a rotary kiln incinerator treating medical waste. Although the devised mass-balance-based approach is of general validity, practical implementation issues should be specifically addressed when dealing with different technologies (e.g., moving grate furnaces) and different feedstocks (e.g., municipal solid waste, MSW). In particular, for MSW, higher time variability of combustion behaviour compared to that observed for medical waste can be expected and a higher time resolution of FGFR measurement might be required.

4. Conclusions

In this paper we discussed a novel methodology to determine the flue gas flow rate in the post-combustion chamber of a waste incinerator. This methodology is based on the measurement of the gas velocity at the boiler exit, where the gas temperature allows direct velocity data acquisitions, and the use of flue gas composition data (CO_2, O_2 and H_2O concentrations) upstream and downstream of the boiler, to derive an estimate of the flue gas flow rate in the post-combustion section by means of a mass balance. The proposed method was validated through a massive experimental campaign on a full-scale medical-waste plant. The aim of the experimental campaign was threefold: 1) experimentally validate the methodology in a wide range of operative conditions of the plant and its sensitivity to ambient conditions; 2) evaluate the mean residence time of the flue-gas of the plant in the post-combustion chamber and the compliance with the Directive 2010/75/EU; 3) evaluate the feasibility to extend the present methodology towards real-time measurements. The results showed that with the proposed method the infiltration of fresh air, and consequently, the flue gas flow rate were consistently evaluated. The residence time was found to be 2.5 s at the highest waste feed-rate, above the 2 s limit which verified the compliance of the plant with the directive. Finally, we found the velocity profiles in cold sections to be self-similar when scaled with the centerline velocity, thus demonstrating the opportunity to devise a revised algorithm for real-time estimation of the flue gas flow rate in standard operative conditions.

Acknowledgements

The author would like to express his gratitude to doctor Alessandro Rossetti for conducting the preliminary studies related to this campaign. Alessandro Talamelli reports financial support was provided by Essere SPA. Valerio Cozzani reports financial support was provided by Regional Agency for the Environment and Energy Prevention of Emilia-Romagna.

References

Bacci di Capaci, R., Pannocchia, G., Pozzo, A. D., Antonioni, G., & Cozzani, V. (2022). Data-driven models for advanced control of acid gas treatment in waste-to-energy plants. *IFAC-PapersOnLine*, *55*, 869–874. doi:10.1016/j.ifacol.2022.07.554. 13th IFAC Symposium on Dynamics and Control of Process Systems, including Biosystems DYCOPS 2022.

Bendat, J. S., & Piersol, A. G. (2000). *Random Data: Analysis and Measurement Procedures*. John Wiley & Sons, Inc.

Biganzoli, L., Racanella, G., Rigamonti, L., Marras, R., & Grosso, M. (2015). High temperature abatement of acid gases from waste incineration. part i: Experimental tests in full scale plants. *Waste Manage.*, *36*, 98 – 105. doi:10.1016/j.wasman.2014.10.019.

Birgen, C., Magnanelli, E., Carlsson, P., & Becidan, M. (2021). Operational guidelines for emissions control using cross-correlation analysis of waste-to-energy process data. *Energy*, *220*, 119733. doi:10.1016/j.energy.2020.119733.

Caneghem, J. V., Block, C., & Vandecasteele, C. (2014). Destruction and formation of dioxin-like pcbs in dedicated full scale waste incinerators. *Chemosphere*, *94*, 42–7.

Chen, T., xiu Zhan, M., Yan, M., ying Fu, J., yong Lu, S., dong Li, X., hua Yan, J., & Buekens, A. (2015). Dioxins from medical waste incineration: Normal operation and transient conditions. *Waste Manag. Res.*, *33*, 644–651. doi:10.1177/0734242X15593639.

Costa, M., Dell'Isola, M., & Massarotti, N. (2012). Temperature and residence time of the combustion products in a waste-to-energy plant. *Fuel*, *102*, 92 – 105. doi:10.1016/j.fuel.2012.06.043. Special Section: ACS Clean Coal.

Dal Pozzo, A., Guglielmi, D., Antonioni, G., & Tugnoli, A. (2018). Environmental and economic performance assessment of alternative acid gas removal technologies for waste-to-energy plants. *Sustain. Prod. Consum.*, *16*, 202 – 215. doi:10.1016/j.spc.2018.08.004.

Dal Pozzo, A., Lazazzara, L., Antonioni, G., & Cozzani, V. (2020). Techno-economic performance of hcl and so2 removal in waste-to-energy plants by furnace direct sorbent injection. *J. Hazard. Mater.*, *394*, 122518. doi:10.1016/j.jhazmat.2020.122518.

Dal Pozzo, A., Muratori, G., Antonioni, G., & Cozzani", V. (2021). Economic and environmental benefits by improved process control strategies in hcl removal from waste-to-energy flue gas. *Waste Manage.*, *125*, 303–315. doi:10.1016/j.wasman.2021.02.059.

De Greef, J., Villani, K., Goethals, J., Van Belle, H., Van Caneghem, J., & Vandecasteele, C. (2013). Optimising energy recovery and use of chemicals, resources and materials in modern waste-to-energy plants. *Waste Manage.*, *33*, 2416 – 2424. doi:10.1016/j.wasman.2013.05.026.

Dzurňák, R., Varga, A., Jablonský, G., Variny, M., Atyafi, R., Lukáč, L., Pástor, M., & Kizek, J. (2020). Influence of air infiltration on combustion process changes in a rotary tilting furnace. *Processes*, *8*, 1292. doi:10.3390/pr8101292.

Eboh, F. C., Åke Andersson, B., & Richards, T. (2019). Economic evaluation of improvements in a waste-to-energy combined heat and power plant. *Waste Manage.*, *100*, 75 – 83. doi:10.1016/j.wasman.2019.09.008.

Eicher, A. R. (2000). Calculation of combustion gas flow rate and residence time based on stack gas data. *Waste Manage.*, *20*, 403–407. doi:10.1016/S0956-053X(99)00342-6.

EN 14790/17 (2017). *Stationary source emissions, Determination of the water vapour in ducts, Standard reference method*.

EN 16911/13 (2013). *Stationary source emissions, Manual and automatic determination of velocity and volume flow rate in ducts* .

Fiorini, T., Segalini, A., Bellani, G., Talamelli, A., & Alfredsson, P. H. (2017). Reynolds stress scaling in pipe flow turbulence first results from CICLoPE. *Philos. Trans. R. Soc. A*, *375*, 20160187. doi:10.1098/rsta.2016.0187.

Kalpakli, A., Örlü, R., & Alfredsson, P. (2013). Vortical patterns in turbulent flow downstream a 90° curved pipe at high Womersley numbers. *Int. J. Heat Mass Transf.*, *44*, 692–699. doi:10.1016/j.ijheatfluidflow.2013.09.008.

Keeling, R., & Manning, A. (2014). Studies of recent changes in atmospheric o2 content. In *Treatise on Geochemistry: Second Edition* (pp. 385–404).

Klopfenstein Jr, R. (1998). Air velocity and flow measurement using a pitot tube. *ISA Trans.*, *37*, 257 – 263. doi:10.1016/S0019-0578(98)00036-6.

Liu, J., Luo, X., Yao, S., Li, Q., & Wang, W. (2020). Influence of flue gas recirculation on the performance of incinerator-waste heat boiler and nox emission in a 500 t/d waste-to-energy plant. *Waste Manage.*, *105*, 450 – 456. doi:10.1016/j.wasman.2020.02.040.

Lueker, T. J., Keeling, R. F., & Dubey, M. K. (2001). The oxygen to carbon dioxide ratios observed in emissions from a wildfire in northern california. *Geophysical research letters*, *28*, 2413–2416.

Magnanelli, E., Tranås, O. L., Carlsson, P., Mosby, J., & Becidan, M. (2020). Dynamic modeling of municipal solid waste incineration. *Energy*, *209*, 118426. doi:10.1016/j.energy.2020.118426.

Poggio, A., & Grieco, E. (2010). Influence of flue gas cleaning system on the energetic efficiency and on the economic performance of a wte plant. *Waste Manage.*, *30*, 1355 – 1361. doi:10.1016/j.wasman.2009.09.008.

Seibt, U., Brand, W., Heimann, M., Lloyd, J., Severinghaus, J., & Wingate, L. (2004). Observations of o2: Co2 exchange ratios during ecosystem gas exchange. *Global Biogeochemical Cycles*, *18*.

Stålnacke, O., Zethraeus, B., & Sarenbo, S. (2008). Experimental method to verify the real residence-time distribution and temperature in MSW-plant. *IFRF Combust. J.*, .

Viganò, F., & Magli, F. (2017). An optimal algorithm to assess the compliance with the T2s requirement of Waste-to-Energy facilities. *Energy Procedia*, *120*, 317–324. doi:10.1016/j.egypro.2017.07.225.

Willert, C. E., Soria, J., Stanislas, M., Klinner, J., Amili, O., Eisfelder, M., Cuvier, C., Bellani, G., Fiorini, T., & Talamelli, A. (2017). Near-wall statistics of a turbulent pipe flow at shear Reynolds numbers up to 40 000. *J. Fluid Mech.*, *826*, R5. doi:10.1017/jfm.2017.498.

Experimental assessment of an indirect method to measure the post-combustion flue gas flow rate in waste-to-energy plant based on multi-point measurements☆

Bellani G.[a,b], Lazzarini L.[a,b], Dal Pozzo A.[c], Moretti S.[e], Zattini M.[d], Cozzani V.[c], Talamelli A.[a,b]

[a] Dipartimento di Ingegneria Industriale, Università di Bologna, Forlì, Italy
[b] Centro Interdipartimentale di Ricerca Industriale aerospaziale, Università di Bologna, Forlì, Italy
[c] Dipartimento di Ingegneria Civile, Chimica, Ambientale e dei Materiali, Università di Bologna, Bologna, Italy
[d] Essere S.p.A., Gruppo Ecoeridania, Forlì, Italy
[e] Arpae Emilia Romagna, Italy

Abstract

In waste-to-energy plants, the determination of the flue gas flow rate in the post-combustion section is of the utmost importance, e.g., for the verification of the compliance to the minimum residence time requirements ($t_{res} > 2s$) or for the control of flue gas treatment reactant injection, but the harsh conditions (high temperature and content of pollutants) do not allow for a direct measurement. The present work reports an experimental assessment of an indirect approach to estimate the flue gas flow rate in the post-combustion section of a rotary kiln plant with reduced uncertainty. This method consists on the direct measurement of the flow rate at a "colder" section of the plant (the boiler outlet) combined to the simultaneous measurements of flue gas composition measurements upstream and downstream of the boiler. From these measurements it is then possible to determine the mass of false air and to retrieve the actual flue gas flow-rate in the post-combustion chamber. A massive experimental campaign has been conducted at a full-scale medical waste incinerator, in which flue gas flow rate was estimated at different waste loads and ambient conditions. The results show that

the percentage of false air can be significant and simply neglecting it can lead to substantial under-performance of the plant. Issues related to the practical implementation of the methods are illustrated in detail and the possibility to extend the methodology towards an online determination of post-combustion flue gas flow rate is discussed.

Keywords

Waste combustion, Fluid dynamics, residence time, Experimental campaign, PCDD

1. Introduction

Increasing restrictions on emissions and more ambitious targets on energy recovery are driving waste-to-energy (WtE) plants towards higher levels of process optimization (De Greef et al. 2013); (Eboh et al. 2019,Liu et al. 2020). To this purpose, modern facilities typically collect hundreds of process data via a wide array of sensors and measuring devices (Birgen et al. 2021). The diffusion of data mining approaches has significantly improved the capability to harness this wealth of information to improve the control of process operation (Bacci di Capaci et al. 2022, Dal Pozzo et al. 2021, Magnanelli et al. 2020).

In this framework, a quantity of great interest is the flue-gas flow-rate (FGFR) generated by waste combustion in the chamber of a grate furnace or in the post-combustion chamber of a rotary kiln. The latter is of special interest because of the restrictive norms that regulate the residence time of the flue-gas. In terms of process control, having an accurate direct or indirect online measurement of the FGFR may significantly improve the control of the feed-rate of reactants injected directly in the combustion chamber for flue gas cleaning, e.g. the furnace injection of dolomitic sorbents (Biganzoli et al. 2015, Dal Pozzo et al. 2020). With respect to the compliance to environmental regulations, in Europe a minimum residence time of 2 s at 850°C is required for flue gas resulting from waste incineration (Directive 2010/75/EU), to ensure the full thermal destruction of organo-halogenated compounds either released by the waste or formed in low-temperature spots during combustion (Chen et al. 2015; Caneghem et al. 2014). Clearly enough, in order to monitor the compliance with this requirement, FGFR needs to be evaluated.

Measurement of WtE FGFR is mandatory at the stack of the plant, but this value might significantly differ from the FGFR generated in the combustion chamber as a consequence of air infiltration in the boiler and in the flue gas cleaning line (Dzurňák et al. 2020). Further uncertainties may derive from the variation in the water vapour concentration in flue gas, depending on the use of wet techniques for flue-gas treatment (Dal Pozzo et al. 2018, Poggio & Grieco 2010). One possible approach is to simply disregard this contamination and make a conservative estimation of the residence time based on stack data. However, if the extent of false air is significant, this assumption can be overly conservative and it can lead to a sub-optimal management of the plant and/or, ultimately to tensions between the plant operator, the regulator and the public opinion.

Unfortunately, a direct measurement of flowrate at the exit of combustion chamber is generally not possible, as the standardized method based on a grid of point velocity measurements made with Pitot tubes (EN 16911/13 2013) is unfeasible due to the extremely high temperatures and harsh conditions of this section of the plant (Klopfenstein Jr 1998). Even the aforementioned Directive 2010/75/EU, while stating that the residence time requires appropriate verification, does not provide indication on how such determination should be performed (Stålnacke et al. 2008).

In industrial practice, monitoring of residence time relies upon semi-empirical algorithms implemented in the Distributed Control System (DCS) that derive local variables from measurements obtained downstream in the flue-gas cleaning line (Costa et al.

2012). For example, Eicher 2000 proposed a procedure to estimate gas-phase residence time in the combustion chamber based only on the combustion chamber temperature and stack-gas data. However, such algorithms are not standardized (Viganò & Magli 2017) and, in order to give reliable estimates, they require calibration data obtained by ad-hoc full-scale test runs on the operating plant.

The aim of the present study is to assess a methodology to determine the FGFR of the post-combustion chamber of a rotary kiln hazardous waste incinerator through a massive experimental campaign on a full-scale medical-waste plant. The data collected in this campaign allows us to quantify the amount of false-air infiltration and its relevance for the overall estimation of flue-gas flow rates of the plant. The proposed method is based on the measurements of the main volumetric composition of the gas (*i.e.* mainly CO_2, O_2 and H_2O) and on the gas velocity downstream of the post-combustion chamber, at the exit of the boiler section, where the gas temperature allows direct velocity measurements. The concentration data are then elaborated to derive the flow-rate corrections from mass balance of the main volumetric components of the gas. In this paper we discuss the theoretical framework of the method, the methodology for its practical implementation and the data from the validation campaign in a full-scale medical-waste plant operating at load and ambient conditions covering the entire operative range. In light of these results, we discuss the potential application of this method to online FGFR estimation based on the available plant data.

2. Material and methods

2.1. Reference case

The case-study presented here is the experimental validation of an indirect method to determine the mass flow rate of the flue gas in the post-combustion chamber of an hazardous waste incinerator with rotary kiln. Figure 1a shows the typical configuration of the combustion and heat recovery section of this type of WtE plant.

As shown in the figure, the post-combustion chamber is positioned immediately after the kiln. The flue gas leaving the post-combustion chamber (section 1 in Figure 1a) enters the steam generator (heat-recovery section of the plant). Here, the gas temperature typically decreases from $1000^{\circ}C$ to about $200 - 250^{\circ}C$. Downstream of the steam generator (section 2 in Figure 1a), the cold gas flows freely in a regular duct before entering the next flue gas treatment sections. If the circuit were perfectly sealed, flue gas flow rate and residence time in the post-combustion chamber could be directly estimated via mass flow measurements in section 2. However, due to constructions constraints, infiltration of ambient air typically occurs in the steam generator, therefore mass-flow measurements in section 2 are biased and typically lead to a substantial overestimation of the mass-flow in the post-combustion chamber.

Here we introduce a correction method based on the mass balance evaluated thanks to the simultaneous measurements of gas volume-fractions at the upstream and downstream end of the steam generator, as well as the experimental procedure to experimentally evaluate this correction.

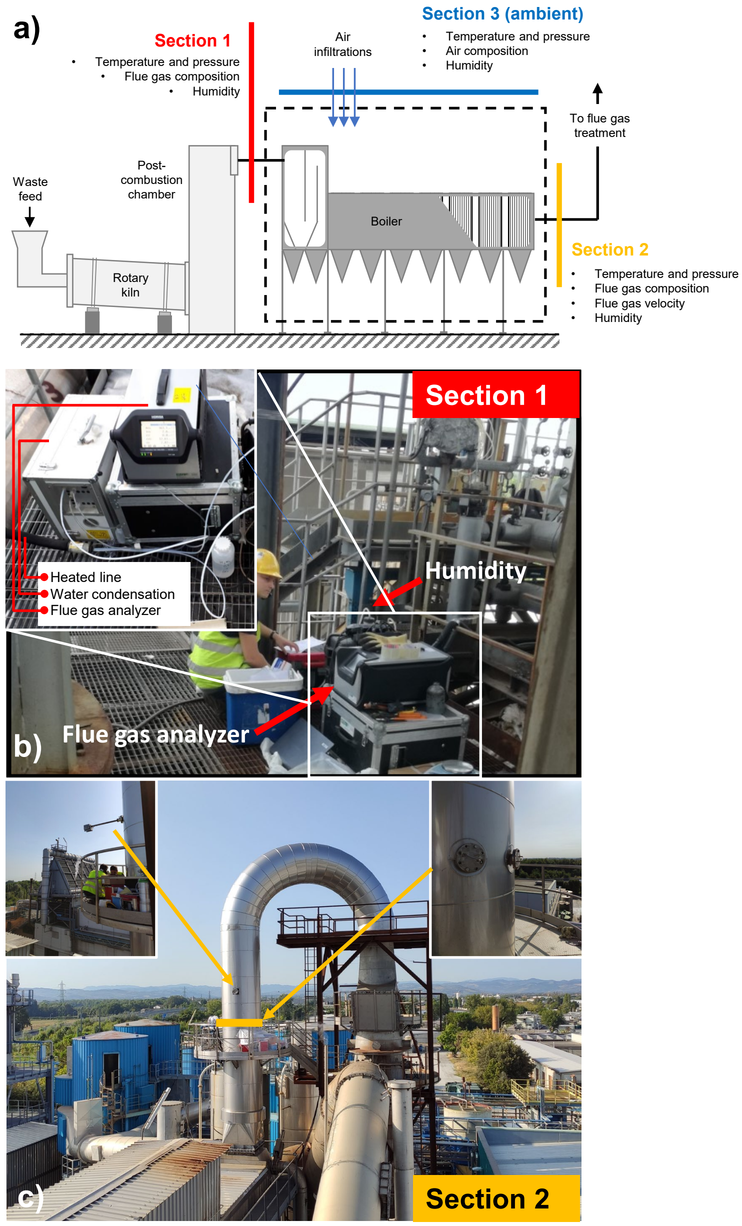

Figure 1: (a) Schematic the incinerator layout: waste enters on the bottom left inside the rotary kiln, at the top of the post-combustion chamber temperatures of the flue gas reach up to $1000^\circ C$; measurement section 2 is placed after the steam generator and the upward 90° corner, here flue gas temperature decreases approximately to $200 - 250^\circ C$; Section 3 indicates ambient condition as close as possible to the post-combustion chamber.(b) Instrumentation placed in section 1. In the inset it can be seen the gas analyzer used to monitor flue gas concentration and the humidity sensor (c) location of the control point and of the measurement grid in section 2 is highlighted by the yellow arrows; red arrows indicates the flue gas direction.

2.2. Methodology

The method is based on the following procedure: a) evaluation of the gas flow rate in the "cold" section (section 2 in Figure 1a); b) measurement of the composition of the flue gas in section 1 and section 2, measurement of the ambient condition in section 3; c) solution of the mass balance in the boiler based on the measurements of gas composition and quantification of the correction term for the indirect estimate of the gas flow rate in the "hot" section (section 1 in Figure 1a). More specifically, once obtained volumetric flow rate in section 2, the mass-balance based on the volumetric concentration measurements in sections 1 (post-combustion), 2 (cold section) and 3 (ambient) can be written as:

$$\dot{m}_1 = \dot{m}_2 - \dot{m}_3, \tag{1}$$

which is convenient to express in terms of volumetric flow-rate and density:

$$\rho_1 \dot{Q}_1 = \rho_2 \dot{Q}_2 - \rho_3 \dot{Q}_3. \tag{2}$$

Writing the balance separately for the components O_2 and CO_2 in the dry flue gas the following system is obtained:

$$\begin{cases} \dot{Q}_{1d}\left[\frac{p_1}{RT_1}(M_{O_2}\varphi_{1,O_2})\right] = \dot{Q}_{2d}\left[\frac{p_2}{RT_2}(M_{O_2}\varphi_{2,O_2})\right] \\ \qquad\qquad -\dot{Q}_{3d}\left[\frac{p_3}{RT_3}(M_{O_2}\varphi_{3,O_2})\right] \\ \dot{Q}_{1d}\left[\frac{p_1}{RT_1}(M_{CO_2}\varphi_{1,CO_2})\right] = \dot{Q}_{2d}\left[\frac{p_2}{RT_2}(M_{CO_2}\varphi_{2,CO_2})\right] \\ \qquad\qquad -\dot{Q}_{3d}\left[\frac{p_3}{RT_3}(M_{CO_2}\varphi_{3,CO_2})\right] \end{cases}$$

Solving now the system for $\dot{Q}_{1d}$ it is possible to obtain the dry volumetric flow rate of the flue gases in section 1:

$$\dot{Q}_{1d} = \dot{Q}_{2d} \left[\frac{\frac{p_2}{T_2}(\varphi_{2,O_2}\varphi_{3,CO_2} - \varphi_{3,O_2}\varphi_{2,CO_2})}{\frac{p_1}{T_1}(\varphi_{1,O_2}\varphi_{3,CO_2} - \varphi_{3,O_2}\varphi_{1,CO_2})} \right], \tag{3}$$

where the term in square brackets represents the correction term due to ambient air infiltration as determined by the differences in volume concentrations and thermodynamic variables (namely pressure and temperature). In order to obtain the wet volumetric flow rate, the vapour fraction φ_{1,H_2O} in the duct must also be taken into account. Thus the expression for the wet volumetric flow rate can be computed as:

$$\dot{Q}_{1,w} = \dot{Q}_{1,d} \frac{100}{100 - \varphi_{H_2O,1}}; \tag{4}$$

Once the wet volumetric flow-rate has been computed, the mean residence time of the flue gases in the post-combustion chamber (t_{res}) can be expressed as:

$$t_{res} = \frac{V_{PC}}{\dot{Q}_{1,w}}, \tag{5}$$

where V_{PC} is the effective volume of the post-combustion chamber.

2.3. Experimental setup and procedure

The methodology outlined in section 2.2, derived from fundamental conservation laws, requires the experimental evaluation of the flue gas flow rate in section 2 ($\dot{Q}_{2d}$) and of temperature, pressure, and concentration of O_2, CO_2, H_2O in sections 1, 2 and 3 (ambient conditions). The determination of these quantities in the operating conditions of a WtE plant poses specific challenges.

In particular, the first challenge concerns the evaluation of $\dot{Q}_{2d}$. Assuming a circular duct, gas flow rate in section 2 is defined from the following double integral:

$$\dot{Q}_{2d} = \int_0^{2\pi} \int_0^r v_c(r, \Theta) dr \cdot r d\Theta \cdot (1 - \varphi_{2,H_2O}) \tag{6}$$

where $\dot{Q}_{2d}$ is the gas flow rate in section 2, dry; r is the radius of the pipe line; $d\Theta$ represent the chosen polar coordinate and v_c is the measured velocity of the flue gases. The coefficient $(1 - \varphi_{H_2O,2})$ accounts for the wet volume fraction $(\varphi_{H_2O,2})$ in section 2.

The directive UNI EN 16911/13 (EN 16911/13 2013) requires that flow-rate measurements must be performed at a straight circular duct sufficiently long (at least 7 diameters: minimum 5 upstream and 2 downstream of the measurement section) to guarantee nearly uniform and symmetric velocity profiles at measurement location. In this condition, the directive requires to measure the velocity at 7 measurement points along 2 diameters.

However, this is not always available in operating plants. This means that velocity profiles may present substantial asymmetries (Kalpakli et al. 2013) and evaluating $\dot{Q}_{2d}$ on a standard course grid may be a significant source of inaccuracies. Therefore, a correct evaluation of $\dot{Q}_{2d}$ requires the acquisition of the flue gas velocity in multiple points, an operation that requires a significant amount of time. For the time needed to measure the velocity in each point of the grid, the plant needs to be operated at a constant feed rate of waste, in order to maintain a relatively constant flow rate of the flue gas.

On the other hand, the other variables required by the methodology (temperature, pressure and concentrations in eq.(3)) need to be evaluated at higher rates for statistical reasons (see section 2.4). In general, their measurements might not be synchronized with the velocity measurements, thus a well-defined interpolation and averaging procedure needs to be defined. In this work, a dedicated experimental campaign at a full-scale plant was carried out to test specific solutions to the aforementioned technical challenges and to validate the proposed methodology.

The experimental campaign was conducted at the medical waste incinerator "Essere S.p.A," in Forlì (Italy). The plant has the layout in Figure 1a. The rotary kiln for waste combustion is followed by a 125 m^3 cylindrical adiabatic post-combustion chamber. The flue gas that leaves the chamber at temperatures of about 1000 $°C$ (first measurement section, S1, on top of the chamber) enters a 11.18MW steam generator. The steam generator is 25 m long and kept at lower than atmospheric pressure to avoid flue gas leakage. As a consequence, as discussed before, ambient air can penetrate from the exterior and mix with the flue gas, increasing its O_2 concentration and decreasing its CO_2 concentration. At the boiler exit the flue gas has cooled to approximately 250 $°C$ and enters a vertical circular duct through an upward 90-degrees corner. The second measurement section (S2) is placed 2.7 diameters downstream this corner and ≈ 2.5 diameters upstream of the 180-degree corner (see figure 1). This section is the closest zone to the post-combustion chamber which presents flow condition that allows direct measurements of differential pressure through a standard Pitot-s probe. In principle, the method of flue gas flowrate estimate based on the mass balance introduced in section 2.2 can be applied using any downstream section of the flue gas line as section S2. The choice to remain closest to the post-combustion chamber was made to avoid other interferences on flue gas composition, other than air infiltrations, that take place downstream in the flue gas cleaning line and can add uncertainty to the estimate of the correction term in eq.(3). For the reference plant, such interferences included changes in water vapour content due to wet scrubbing for HCl/SOx removal and, to a lesser extent, changes in CO2 concentration due to uptake by hydrated lime injected for HCl removal Dal Pozzo et al. 2018.

Although the conditions in S2 are closest to the one imposed by the standard UNI-

EN 16911/13 2013, it is well known that a 90-degree corner produces strong asymmetry in the flow (Kalpakli et al. 2013). To account for this, an higher resolution for the acquisition of velocity data was pursued and a refined measurement grid of 44 logarithmically-spaced points on 4 evenly spaced diameters was adopted (see Fig.2a). For each grid point, the flue gas velocity measured with a Pitot-S was sampled for 15 s. This time was chosen to minimize statistical uncertainty while keeping the total measurement time below 60 min, a duration in which it was possible to operate the plant at a reasonably constant flue gas flow rate. To monitor the stability of the flue gas flow rate during the measurement, a second Pitot-S probe was positioned at the center of the duct, 1 m downstream of S2 (control point). The position of the probes are manually controlled through specifically designed flanges.

At sections S1 and S2, as well as in ambient air outside the steam generator (S3), pressure, temperature, O_2 and CO_2 concentrations were monitored at a rate of one sample per minute for the entire duration of the experiments. Pressure was measured with a differential pressure transducer (2.5 kPa range, 1% full-scale accuracy). The temperature sensor is a k-type thermocouple of 0-1200 °C range for section 1, whereas j-type thermocouple for sections 2 and 3. The concentrations of CO_2 and O_2 in the dry gas were measured by non-dispersive infrared absorption and paramagnetic method, respectively. Finally, the average volumetric concentration of water vapor in the gas was measured in all sections for each experiment by the standard condensation/absorption technique (EN 14790/17 2017). The sampling time of each instrument was set to be larger than their respective time-response. Data-rates, instrument types and relative accuracy are summarized in table 1.

Parameter	Frequency [Samples/min]	Instrument	Accuracy	Time response
S1				
$\varphi_{1,0_2}$	1	Gas analyzer PG-300 Horiba	$\pm 1\%$	45 s
$\varphi_{1,C0_2}$	1			
φ_{1,H_2O}	single sampe	Gravimetric test	$\pm 3\%$	1 hr
$T1$	1	type k thermocouple	$\pm 1\%$	NA
$p1$	1	Digital stack gas velocity		
S2				
$\varphi_{2,0_2}$	1	Gas analyzer PG-300 Horiba	$\pm 1\%$	45 s
$\varphi_{2,C0_2}$	1			
φ_{2,H_2O}	single sampe	Gravimetric test	$\pm 3\%$	1 hr
$T2$	1	type j thermocouple	$\pm 1\%$	NA
$p2$	1	Digital stack gas velocity		
v_k	manual sampling	Pitot - S	$\pm 1\%$	
v_fC	1			
S3				
$\varphi_{3,0_2}$	1	Gas analyzer PG-300 Horiba	$\pm 1\%$	45 s
$\varphi_{3,C0_2}$	1			
φ_{3,H_2O}	single sampe	Gravimetric test	$\pm 3\%$	1 hr
$T3$	1	type j thermocouple	$\pm 1\%$	NA
$p3$	1	Digital stack gas velocity		

Table 1: Summary of the instrumentation used to measure the relevant parameters with the corresponding sampling frequency, accuracy and time response. The accuracy is the one specified by the instrument manufacturer.

2.4. Data processing and averaging

As discussed in section 2.3, to determine the volumetric flow rate in section 2 we must evaluate the integral as defined by eq. (6). We define the index $k = 1 : 44$ corresponding to the $k-th$ Pitot-S measurement. At each k is associated the corresponding measurement point on the grid and time-interval in which the data is taken.

The velocity of the flue gas v_k is computed as follows:

$$v_k = \sqrt{\frac{2\Delta p_k}{\rho_{2,k}}}, \tag{7}$$

where Δp_k is the k_{th} 15s-average differential pressure measured by the Pitot-S. The variable $\rho_{2,k}$ is the density of the flue gas determined according to the following expression:

$$\rho_{2,k} = \frac{p_k}{RT_k}[M_{O_2}\varphi_{2,k,O_2}+M_{CO_2}\varphi_{2,k,CO_2}+M_{H_2O}\varphi_{2,k,H_2O}+M_{N_2}(1-\varphi_{2,k,O_2}-\varphi_{2,k,CO_2}-\varphi_{2,k,H_2O})], \tag{8}$$

where M_x is the molar mass of the element x, $\varphi_{2,k,x}$ is the volume concentration of the element x measured in S2 at time interval k, p_k and T_k are the local pressure and temperature at time-interval k and R is the molar gas constant equal to 8.31446 expressed in $[J/Kmol]$. The average volume flow rate $\dot{Q}_{S_2}$ is computed by numerically solving the integral of eq. (6) according to the trapezoid rule. Since $\dot{Q}_{2,d}$ represents a single average value of the volume flow-rate over the time interval needed to span the entire grid, the correction term expressed in eq. (3) must be averaged as well. Since the volumetric concentrations are not independent variables, the correction term cannot be computed after averaging the individual terms (Bendat & Piersol 2000) but as global average of the instantaneous combination of each variable, according to the following expression:

$$\dot{Q}_{1d} = \dot{Q}_{2d} \cdot \sqrt{\left[\frac{\frac{p_2}{T_2}(\varphi_{2,O_2}\varphi_{3,CO_2} - \varphi_{3,O_2}\varphi_{2,CO_2})}{\frac{p_1}{T_1}(\varphi_{1,O_2}\varphi_{3,CO_2} - \varphi_{3,O_2}\varphi_{1,CO_2})}\right]}. \tag{9}$$

It must be pointed out that a potential source of uncertainty is given by the time delay between the measurements in S1 and S2. The effect of the time delay is to reduce the correlation coefficient between the quantities measured in S1 and S2, thus altering the balance expressed in eq.(9). However, in the present configuration, the estimated time-delay is between 1-3 s for all cases, which is much smaller than both the sampling interval and the characteristic time-scales of the flow. Therefore, it can be considered negligible. This is also confirmed by the fact that the correlation coefficient of the corresponding signals is found to be between 0.6 and 0.9 in all cases. More details on the choices of sampling parameters, measurement grids and associated experimental uncertainties are given in the supplementary material.

2.5. Experimental campaign

In order to test the methodology over a wide range of operating conditions of the plant and extract relevant trends, experiments were performed at three different levels of waste loading, corresponding to the lowest (Low: ≈ 2700 kg/h), intermediate (Medium: ≈ 3800 kg/h) and nearly maximum loading (High: ≈ 4800 kg/h) capability of the plant. Each test was at least 1-h long and, in addition to a controlled waste feed rate, also the air feed rate to the kiln was maintained as constant as possible during the tests to reduce its influence in the estimate of the FGFR. To test the robustness of the results in different ambient conditions, the same three cases were repeated at 6 months interval from each other (in summer and winter). Therefore, we have divided the results in 6 test cases, namely: SL, SM, SH and WH, WM, WL; where L, M and H stands for low, medium and high loading conditions, respectively, while S and W indicate summer and winter sessions, as shown in table 2.

3. Results and discussion

Case	Load $[kg/h]$	$Q_{2,d}$ $[m^3/s]$	$Q_{2,w}$ $[m^3/s]$	Q_2 $[Nm^3/h]$	φ_{2,H_2O} [%]	$Q_{1,d}$ $[m^3/s]$	$Q_{1,w}$ $[m^3/s]$	Q_1 $[Nm^3/h]$	φ_{1,H_2O} [%]	t_{res} $[s]$
SL	2700	14.20	17.30	34512	17.88	27.61	34.54	26759	20.05	$3.62 \pm 2.74\%$
WL	2868	13.10	15.23	30742	13.97	26.85	31.99	23723	16.08	$4.06 \pm 2.72\%$
WM	3770	15.62	19.30	38081	19.06	26.51	33.72	25821	21.36	$3.71 \pm 2.66\%$
SM	3910	17.03	18.87	36420	NA	*29.87	*36.40	NA	NA	$*3.14 \pm 2.70\%$
SH1	4684	20.15	23.31	43705	NA	*33.20	*40	NA	NA	$*2.70 \pm 2.63\%$
SH2	4700	19.49	23.51	44310	17.08	36.12	44.93	34374	19.61	$2.78 \pm 2.59\%$
WH	4770	19.15	22.67	42930	15.53	34.69	42.90	30412	19.12	$2.91 \pm 2.74\%$

Table 2: Loading conditions and estimated flow rates for each of the six different tested conditions; $\dot{Q}_{2,d}$ and $\dot{Q}_{2,w}$ shows respectively the dry and wet gas flow rate measured in section 2, $\dot{Q}_2$ represent the FGFR in standardized condition; $\dot{Q}_{1,d}$ and $\dot{Q}_{1,w}$ represents respectively the dry and wet gas flow rate evaluated in post combustion chamber; $\dot{Q}_1$ shows the FGFR in standardized condition; φ_{i,H_2O} show the humidity for sections 2 and 1 respectively; t_{res} shows the residence time of the flue gas in post-combustion chamber. The cases SM and $SH1$ have been discarded because of incoherent data. The case SH has been repeated in order to obtain valid data at the highest loading condition. The sub-indexes $SH1$ and $SH2$ have been introduced to identify the discarded and the valid test, respectively; *, NA:data acquired during tests SM and SH1 were recovered using the mean infiltration coefficient and the mean humidity values measured in the remaining experimental campaigns.

3.1. Data assessment and validation

Given the challenging conditions in which the experiments are performed (*i.e.* extreme temperature, corrosive gas, dust particles, unknown fuel composition, etc) a careful preliminary assessment of the consistency of the data is needed. The first assessment concerns the hypothesis of statistical stationariety of the plant conditions. This is done by analyzing the timeseries of the velocity measured at the control point, looking for possible trends or anomalous fluctuations indicating for non-stationariety of the plant operating conditions.

Figure 2(c) shows a time trace of the control point for one of the cases. Analysis of the time-series for all cases show that despite the variability of the fuel composition during each test, the plant operates at reasonably constant conditions since no significant trends or bursts are observed. Furthermore, the standard deviation of the velocity fluctuations normalized by the value of the local mean are within 5%, a value that is comparable with the expected level of turbulent fluctuations in the centre of a circular duct (Fiorini et al. 2017; Willert et al. 2017). Given the stationary conditions of the plant, the next step of the procedure is the calculation of the gas flow rate in section 2 by integration of the velocity profiles along the diameters shown in figure 2a.

Considering that the measurement section is located downstream of a 90° bend, the flow is not expected to be canonical (*i.e.* fully-developed pipe flow), therefore, there are no analytical or empirical formulas to describe the expected velocity profiles. However, it is well known that in a corner the radial pressure gradient produces strongly asymmetric profiles except in the direction parallel to the rotation axis (D1 in the present case)(Kalpakli et al. 2013). Figure 2c shows that the measured profiles are consistent with the expected behaviour.

Furthermore, velocity profiles scaled by the centerline velocity or by the average velocity are expected to have a substantially self-similar shape (i.e. independent of

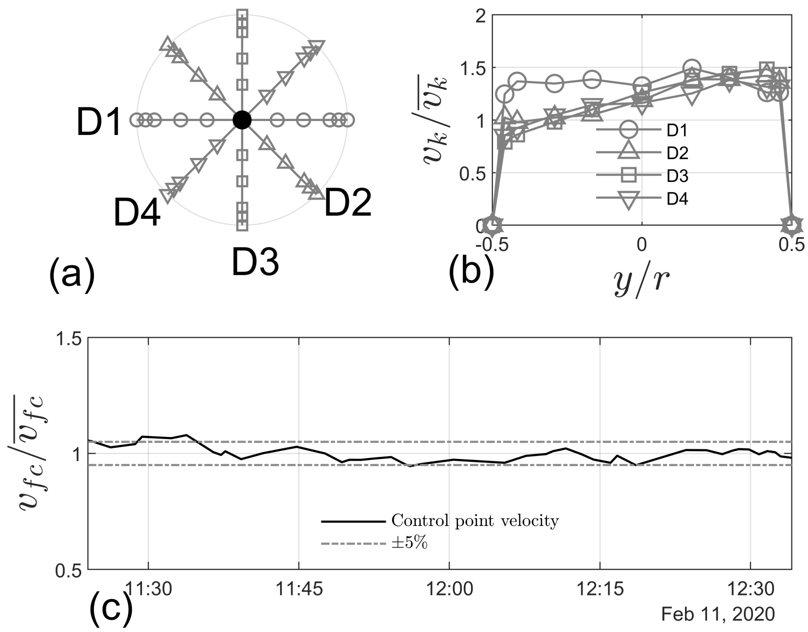

Figure 2: (a) represents the measurement grid used in S2, each diameter has 9 measurement points spaced logarithmically from the wall to the center line. The physical coordinates of the measurement points expressed as a fraction of the duct radius are: -0.4583, -0.4167, -0.2917, -0.1667, 0, 0.1667, 0.2917, 0.4167, 0.4583. the central black dot shows the position of the control point placed 1 meter downstream with respect to the measurements grid; (b) depict the shape of the velocity profiles measured starting from D1 to D4 and normalized with the mean velocity of the entire test, the dimension of each symbols reflects the actual standard deviation associated to the correspondent measurement point; the mean value of the standard deviation is of the order of 6-7% (c) shows the behaviour of the control point velocity during a winter test normalized with the mean velocity of the entire test.

the average speed itself). This normalization allows us to compare profiles related to different flow conditions and to compute mean scaled velocity profiles for the winter and summer sessions averaging the corresponding profiles for the three cases of each season. These averaged velocity profiles are shown and compared in figure 3. The substantial agreement between the two sessions is an indication of the consistency of the experimental procedure.

The final assessment is done on the gas volumetric composition data. These measurements are especially challenging in section S1 due to the highly aggressive environment. In these section, partial probe occlusions (e.g., by deposition and melting of

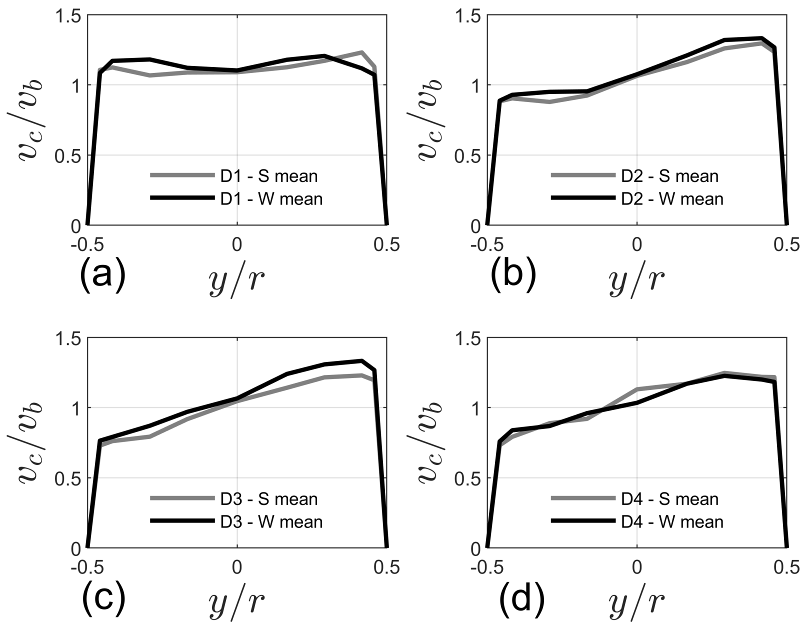

Figure 3: Normalized (with bulk velocity and pipe radius) mean velocity profile divided in diameters; D1 in figure (a), D2 in figure (b), D3 in figure (c) and D4 in figure (d), in grey the summer experiments whereas in black the winter experiments.

combustion fly ash) can cause significant biases in the measurements, therefore a check of the consistency of these measurements is essential. To this purpose, we impose a constraint based on a mass balance between CO_2 and O_2. The concentration of these two species in the flue gas from combustion processes is anti correlated, as combustion consumes O_2 and produces CO_2 according to an exchange ratio or oxidative ratio (defined as $-\Delta O_2\ /\Delta CO_2$) that depends on the elemental composition of the fuel (Seibt et al. 2004). Such ratio lies in the range $1.1 - 1.3$ for solid fuels of diverse nature (Keeling & Manning 2014; Lueker et al. 2001). Therefore, even if the waste composition fed to the incinerator is relatively heterogeneous, it was found that for most of the data collected during the experimental campaign the volumetric concentration of CO_2 plotted against that of O_2 returned a linear correlation (see Figure 4), corresponding to an average oxidative ratio of 1.25. Notably, the data from two tests (SM and SH1), indicated by the gray triangles deviated significantly from the trend, pinpointing a possible instrumental error. Given that a reliable determination of the volumetric concentrations is key for the entire procedure, these cases were marked as "discarded" cases. The SH case was repeated after the probe had been cleaned from occlusions and the following measurements show good agreement with the expected trend (see diamonds in the figure).

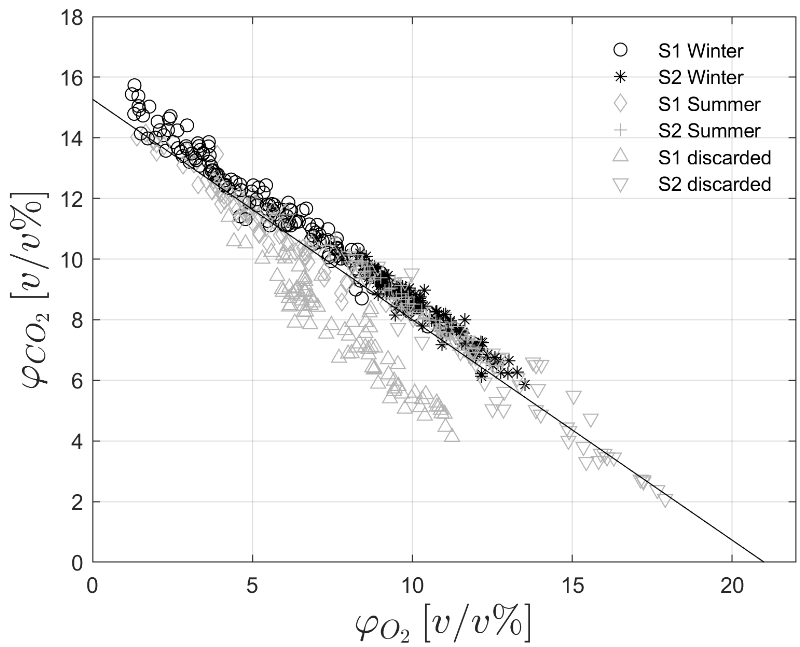

Figure 4: Volumetric gas composition, CO_2 Vs. O_2. Each point represents a measurement conducted during the tests (time resolution 60 s) The black circles represent the winter data in S1, the grey diamonds represent the summer data in S1, the black asterisks represent the winter data in S2, the grey cross represents the summer data S2, the gray triangles represent discarded data due to instrumentation fault in S1.

3.2. Flow-rate measurements

Once the data have been validated, it is possible to proceed with the numerical integration of the velocity profiles measured in S2 in order to determine the dry volumetric flow rate of the flue gases, as defined in equation 6. Figure 5 (a) shows the measured dry flow rate values in S2 plotted against the waste feed-rate. The figure shows a nearly-linear increasing trend as the waste feed-rate increases. For the purpose of estimating the repeatability of the measurements, also the cases who did not pass the validation of the volumetric concentration measurements were included, since these did not affect the measurement of $Q_{2,d}$. It can be noticed a substantial agreement between summer and

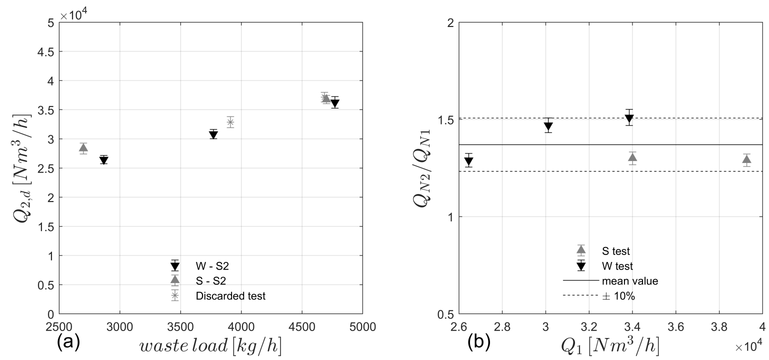

Figure 5: (a) Dry gas flow rate in section 2. Summer and winter tests are shown by black and grey symbols, respectively. The grey asterisk symbols are the discarded cases (SM1 and SH1). Error bars is the estimated measurements uncertainty. (b) Infiltration coefficient expressed using mass flow rate in S1 and S2. black downward triangles represents the winter experiments, grey upward triangles represents the summer experiments, black line highlight the mean value of the coefficient while dashed black lines shows a ±10% with respect to the mean value.

winter measurements, especially at medium and high waste load, while a slightly larger scatter is present at low load. Considering that waste is a highly heterogeneous fuel, it can be expected that at low waste feed rates the statistical variability in combustion behaviour given by different waste fractions is magnified.

In order to evaluate flow rate in S1 the infiltration through the steam generator needs to be quantified according to equation 9. Figure 5 (b) shows the infiltration coefficient expressed as the ratio between Q_{2N}/Q_{1N} where Q_{2N} and Q_{1N} represent the volume flow rates in S2 and S1, respectively, with density at standard air conditions.

The mean value of the infiltration coefficient is of 1.38 $\pm 10\%$. This value shows that the amount of false air entrained in the boiler section only is hardly negligible being nearly 40% of the total mass flow rate. This percentage increases even more if the volume-flow rate (to which the residence times are proportional) is considered, given the density ratio between the cold section and the post-combustion chamber.

The higher extent of variation of the infiltration coefficient observed in winter can be explained by the fact that the scheduled annual maintenance of the steam generator was carried out just before the summer tests. Therefore, the winter tests were done in presence of an higher degree of fouling and occlusions in the boiler, which is compatible with a higher duty for the induced-draft fan and thus to a higher differential pressure. This condition is therefore compatible with the higher value of dilution observed.

3.3. Residence time

Figure 6a shows that the trend observed for Q_{S2} is confirmed also by the wet volumetric flow rate, computed according to equations (3) and (4). The asterisks in the figures are the cases originally discarded because of unreliable flue gas composition measurements and humidity measurements. For these cases, it was not possible to directly compute the infiltration coefficient, therefore, instead of the direct measurement, the mean value of the measured coefficients (*e.g.* 1.38) has been taken. The same approach was followed for the humidity, as the mean value of the humidity measured in all cases in S2 and S1 respectively, was used. The resulting flow-rates follow remarkably well the trend of the measured values.

In order to check if the measured values are consistent with the plant design, it is interesting to convert $Q_{1,w}$ into residence times according to eq. (5). The reference volume used for this calculation is of $125.1\, m^3$. Based on this expression, the evolution of residence time as a function of the plant waste-loading is shown in figure 6 (b); The

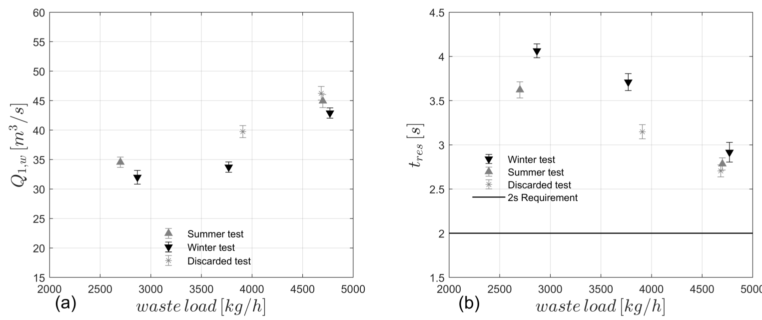

Figure 6: (a) wet gas flow rate calculated for S1, (b) t_{res} of the flue gas in post-combustion chamber. grey error-bar represents summer experiments, black error-bar represents winter experiments, asterisks represents the discarded experiments. These cases have been recovered using the average infiltration coefficient and the average humidity measured in all cases. Black line represents the 2 seconds requirement.

figure shows that as the waste feed rate approaches its design limit (5000 kg/h), the residence time gets close to the two-seconds limit with a margin of about 40% against an estimated uncertainty on the single measure of the order of 2.5% (see supplementary material). Assuming that the plant is designed to respect the norm, the fact that the estimated residence times are close but higher than the prescribed value of 2s at nearly the maximum operative range of the plant can be considered an indirect assessment of consistency of the results obtained in the entire campaign. Furthermore, it is interesting to notice that without the corrections for false air entrainment, given its extent, it may appear that the plant is violating the norm of the 2s residence times, thus a reduced operational range should be imposed.

3.4. Discussion

Despite the simplicity of the theoretical procedure devised to estimate the FGFR in the post-combustion chamber, its experimental implementation implied numerous issues that needed to be addressed with a massive experimental campaign. The main issues were: stability of plant operation during the tests, consistency of the velocity profiles, and reliability of the volumetric concentration measurements in all operating conditions.

Regarding the possibility to operate the plant in stable conditions, the data collected in the control point showed that no significant trends or anomalous bursts were observed. This confirms the main assumption that the flow-rate is statistically stationary during each measured case (as already observed in the preliminary tests, see supplementary material). The stability of the flow conditions is also confirmed by the substantial repeatability of the results over independent measurement sets collected in different period of the year with possible influences of fuel seasonal variability and different ambient conditions (*i.e.* winter and summer season, see fig. (3)).

Another important finding is that the velocity profiles are self-similar when scaled by the radius and the centerline velocity. This finding has two relevant implications: on one hand this can be used to evaluate the accuracy of the individual velocity measurements by looking at the deviation from the overall mean. This was found to be below 10% for all cases, and it reduced to 5% for the cases with an improved control of the S-probe position; Most importantly, self-similarity of the velocity profiles in $S2$ section point at the possibility of estimating the flow-rate from a single-point measurement.

A crucial part of the procedure is the volumetric concentration measurements. A small bias in this measurements can lead to significant errors in the estimation of the FGFR. The diagnostic plot shown in figure 4 has proven to be a robust tool to validate these measurements and produce a consistent estimation of the infiltration of fresh air through the steam-generator. Further work should be done in order to explore the influence of non-ideal burning conditions on the diagnostic plot, and additional checks, such as the correlation coefficients between the four signals could be introduced.

However, the consistency of the present results in terms of infiltration coefficient (see figure 5(b)) and the estimated residence time near to the 2 s limits at the design point of the plant (see figure 6 (b)), obtained in a variety of operating conditions, are encouraging.

The obvious limit of the methodology presented here is that it does not allow obtaining instantaneous FGFR estimates. However, the experimental data presented here provide a solid ground to prospect an extension of the present methodology towards real-time estimation method. In particular, based on the results we can outline the following revised procedure that would require minimal plant modification: a) Exploit self-similarity of velocity profiles to obtain the volumetric flow rate of the cold section with velocity measurements in a single point. b) Estimate an instantaneous or average infiltration coefficient from CO_2 and O_2 online measurements; c) Compute dry volumetric flow rate in the hot section based on the infiltration coefficient; d) Estimate the wet flow rate based on the typical mean value of the water vapour concentration in the flue gas.

Alternatively, a plant operator might consider setting up a different algorithm for real-time FGFR estimate in the post-combustion chamber exclusively based on existing process instrumentation (e.g., estimate from online flue gas composition measurements at stack or from energy balance in the heat recovery section of the plant). Any algorithm for FGFR estimate based on indirect measurements of other variables through existing process instrumentation or ad-hoc sensors would require a training and validation campaign. The present methodology offers the possibility to obtain average estimates of FGFR in the post-combustion chamber under different operating conditions that can be used as the necessary dataset for the training and validation of such algorithms.

Lastly, it is worth recalling that this paper demonstrated the methodology in application to a specific, albeit relevant, case of WtE plant: a rotary kiln incinerator treating medical waste. Although the devised mass-balance-based approach is of general validity, practical implementation issues should be specifically addressed when dealing with different technologies (e.g., moving grate furnaces) and different feedstocks (e.g., municipal solid waste, MSW). In particular, for MSW, higher time variability of combustion behaviour compared to that observed for medical waste can be expected and a higher time resolution of FGFR measurement might be required.

4. Conclusions

In this paper we discussed a novel methodology to determine the flue gas flow rate in the post-combustion chamber of a waste incinerator. This methodology is based on the measurement of the gas velocity at the boiler exit, where the gas temperature allows direct velocity data acquisitions, and the use of flue gas composition data (CO_2, O_2 and H_2O concentrations) upstream and downstream of the boiler, to derive an estimate of the flue gas flow rate in the post-combustion section by means of a mass balance. The proposed method was validated through a massive experimental campaign on a full-scale medical-waste plant. The aim of the experimental campaign was threefold: 1) experimentally validate the methodology in a wide range of operative conditions of the plant and its sensitivity to ambient conditions; 2) evaluate the mean residence time of the flue-gas of the plant in the post-combustion chamber and the compliance with the Directive 2010/75/EU; 3) evaluate the feasibility to extend the present methodology towards real-time measurements. The results showed that with the proposed method the infiltration of fresh air, and consequently, the flue gas flow rate were consistently evaluated. The residence time was found to be 2.5 s at the highest waste feed-rate, above the 2 s limit which verified the compliance of the plant with the directive. Finally, we found the velocity profiles in cold sections to be self-similar when scaled with the centerline velocity, thus demonstrating the opportunity to devise a revised algorithm for real-time estimation of the flue gas flow rate in standard operative conditions.

Acknowledgements

The author would like to express his gratitude to doctor Alessandro Rossetti for conducting the preliminary studies related to this campaign. Alessandro Talamelli reports financial support was provided by Essere SPA. Valerio Cozzani reports financial support was provided by Regional Agency for the Environment and Energy Prevention of Emilia-Romagna.

References

Bacci di Capaci, R., Pannocchia, G., Pozzo, A. D., Antonioni, G., & Cozzani, V. (2022). Data-driven models for advanced control of acid gas treatment in waste-to-energy plants. *IFAC-PapersOnLine*, *55*, 869–874. doi:10.1016/j.ifacol.2022.07.554. 13th IFAC Symposium on Dynamics and Control of Process Systems, including Biosystems DYCOPS 2022.

Bendat, J. S., & Piersol, A. G. (2000). *Random Data: Analysis and Measurement Procedures*. John Wiley & Sons, Inc.

Biganzoli, L., Racanella, G., Rigamonti, L., Marras, R., & Grosso, M. (2015). High temperature abatement of acid gases from waste incineration. part i: Experimental tests in full scale plants. *Waste Manage.*, *36*, 98 – 105. doi:10.1016/j.wasman.2014.10.019.

Birgen, C., Magnanelli, E., Carlsson, P., & Becidan, M. (2021). Operational guidelines for emissions control using cross-correlation analysis of waste-to-energy process data. *Energy*, *220*, 119733. doi:10.1016/j.energy.2020.119733.

Caneghem, J. V., Block, C., & Vandecasteele, C. (2014). Destruction and formation of dioxin-like pcbs in dedicated full scale waste incinerators. *Chemosphere*, *94*, 42–7.

Chen, T., xiu Zhan, M., Yan, M., ying Fu, J., yong Lu, S., dong Li, X., hua Yan, J., & Buekens, A. (2015). Dioxins from medical waste incineration: Normal operation and transient conditions. *Waste Manag. Res.*, *33*, 644–651. doi:10.1177/0734242X15593639.

Costa, M., Dell'Isola, M., & Massarotti, N. (2012). Temperature and residence time of the combustion products in a waste-to-energy plant. *Fuel*, *102*, 92 – 105. doi:10.1016/j.fuel.2012.06.043. Special Section: ACS Clean Coal.

Dal Pozzo, A., Guglielmi, D., Antonioni, G., & Tugnoli, A. (2018). Environmental and economic performance assessment of alternative acid gas removal technologies for waste-to-energy plants. *Sustain. Prod. Consum.*, *16*, 202 – 215. doi:10.1016/j.spc.2018.08.004.

Dal Pozzo, A., Lazazzara, L., Antonioni, G., & Cozzani, V. (2020). Techno-economic performance of hcl and so2 removal in waste-to-energy plants by furnace direct sorbent injection. *J. Hazard. Mater.*, *394*, 122518. doi:10.1016/j.jhazmat.2020.122518.

Dal Pozzo, A., Muratori, G., Antonioni, G., & Cozzani", V. (2021). Economic and environmental benefits by improved process control strategies in hcl removal from waste-to-energy flue gas. *Waste Manage.*, *125*, 303–315. doi:10.1016/j.wasman.2021.02.059.

De Greef, J., Villani, K., Goethals, J., Van Belle, H., Van Caneghem, J., & Vandecasteele, C. (2013). Optimising energy recovery and use of chemicals, resources and materials in modern waste-to-energy plants. *Waste Manage.*, *33*, 2416 – 2424. doi:10.1016/j.wasman.2013.05.026.

Dzurňák, R., Varga, A., Jablonský, G., Variny, M., Atyafi, R., Lukáč, L., Pástor, M., & Kizek, J. (2020). Influence of air infiltration on combustion process changes in a rotary tilting furnace. *Processes*, *8*, 1292. doi:10.3390/pr8101292.

Eboh, F. C., Åke Andersson, B., & Richards, T. (2019). Economic evaluation of improvements in a waste-to-energy combined heat and power plant. *Waste Manage.*, *100*, 75 – 83. doi:10.1016/j.wasman.2019.09.008.

Eicher, A. R. (2000). Calculation of combustion gas flow rate and residence time based on stack gas data. *Waste Manage.*, *20*, 403–407. doi:10.1016/S0956-053X(99)00342-6.

EN 14790/17 (2017). *Stationary source emissions, Determination of the water vapour in ducts, Standard reference method*.

EN 16911/13 (2013). *Stationary source emissions, Manual and automatic determination of velocity and volume flow rate in ducts* .

Fiorini, T., Segalini, A., Bellani, G., Talamelli, A., & Alfredsson, P. H. (2017). Reynolds stress scaling in pipe flow turbulence first results from CICLoPE. *Philos. Trans. R. Soc. A*, *375*, 20160187. doi:10.1098/rsta.2016.0187.

Kalpakli, A., Örlü, R., & Alfredsson, P. (2013). Vortical patterns in turbulent flow downstream a 90° curved pipe at high Womersley numbers. *Int. J. Heat Mass Transf.*, *44*, 692–699. doi:10.1016/j.ijheatfluidflow.2013.09.008.

Keeling, R., & Manning, A. (2014). Studies of recent changes in atmospheric o2 content. In *Treatise on Geochemistry: Second Edition* (pp. 385–404).

Klopfenstein Jr, R. (1998). Air velocity and flow measurement using a pitot tube. *ISA Trans.*, *37*, 257 – 263. doi:10.1016/S0019-0578(98)00036-6.

Liu, J., Luo, X., Yao, S., Li, Q., & Wang, W. (2020). Influence of flue gas recirculation on the performance of incinerator-waste heat boiler and nox emission in a 500 t/d waste-to-energy plant. *Waste Manage.*, *105*, 450 – 456. doi:10.1016/j.wasman.2020.02.040.

Lueker, T. J., Keeling, R. F., & Dubey, M. K. (2001). The oxygen to carbon dioxide ratios observed in emissions from a wildfire in northern california. *Geophysical research letters*, *28*, 2413–2416.

Magnanelli, E., Tranås, O. L., Carlsson, P., Mosby, J., & Becidan, M. (2020). Dynamic modeling of municipal solid waste incineration. *Energy*, *209*, 118426. doi:10.1016/j.energy.2020.118426.

Poggio, A., & Grieco, E. (2010). Influence of flue gas cleaning system on the energetic efficiency and on the economic performance of a wte plant. *Waste Manage.*, *30*, 1355 – 1361. doi:10.1016/j.wasman.2009.09.008.

Seibt, U., Brand, W., Heimann, M., Lloyd, J., Severinghaus, J., & Wingate, L. (2004). Observations of o2: Co2 exchange ratios during ecosystem gas exchange. *Global Biogeochemical Cycles*, *18*.

Stålnacke, O., Zethraeus, B., & Sarenbo, S. (2008). Experimental method to verify the real residence-time distribution and temperature in MSW-plant. *IFRF Combust. J.*, .

Viganò, F., & Magli, F. (2017). An optimal algorithm to assess the compliance with the T2s requirement of Waste-to-Energy facilities. *Energy Procedia*, *120*, 317–324. doi:10.1016/j.egypro.2017.07.225.

Willert, C. E., Soria, J., Stanislas, M., Klinner, J., Amili, O., Eisfelder, M., Cuvier, C., Bellani, G., Fiorini, T., & Talamelli, A. (2017). Near-wall statistics of a turbulent pipe flow at shear Reynolds numbers up to 40 000. *J. Fluid Mech.*, *826*, R5. doi:10.1017/jfm.2017.498.

Declaration of interests

☐The authors declare that they have no known competing financial interests or personal relationships that could have appeared to influence the work reported in this paper.

☒The authors declare the following financial interests/personal relationships which may be considered as potential competing interests:

Alessandro Talamelli reports financial support was provided by Essere SPA. Valerio Cozzani reports financial support was provided by Regional Agency for the Environment and Energy Prevention of Emilia-Romagna.